Journal of Medicinal Chemistry

Article

Design and synthesis of soluble and cell-permeable PI3K# inhibitors for long-acting inhaled administration

Matthew W. D. Perry, Karin Björhall, Britta K. Bonn, Johan Carlsson, Yunhua Chen, Anders Eriksson, Linda Fredlund, Hai'e Hao, Neil S. Holden, Kostas Karabelas, Helena Lindmark, Feifei Liu, Nils Pemberton, Jens Petersen, Sandra Rodrigo Blomqvist, Reed W. Smith, Tor Svensson, Ina Terstiege, Christian Tyrchan, Wenzhen Yang, Shuchun Zhao, and Linda Öster

J. Med. Chem., **Just Accepted Manuscript** • Publication Date (Web): 18 May 2017

Just Accepted

ACS Publications

Journal of Medicinal Chemistry is published by the American Chemical Society. 1155 Sixteenth Street N.W., Washington, DC 20036

	Medicines and Early Development, AstraZeneca Gothenburg, Medicinal Chemistry Tyrchan, Christian; Respiratory, Inflammation and Autoimmunity, Innovative Medicines and Early Development, AstraZeneca Gothenburg, Medicinal Chemistry Yang, Wenzhen; Pharmaron Beijing Co., Ltd. Zhao, Shuchun; Pharmaron Beijing Co., Ltd. Öster, Linda; Discovery Sciences, Innovative Medicines and Early Development, AstraZeneca Gothenburg

Design and synthesis of soluble and cell-permeable PI3Kδ inhibitors for long-acting inhaled administration

Authors Matthew W D Perry,[ab] Karin Björhall,[ad] Britta Bonn,[ac] Johan Carlsson,[e] Yunhua Chen,[f] Anders Eriksson,[ab] Linda Fredlund,[e] Hai'e Hao,[f] Neil S Holden,[ad] Kostas Karabelas,[a] Helena Lindmark,[e] Feifei Liu,[f] Nils Pemberton,[ab] Jens Petersen,[e] Sandra Rodrigo Blomqvist,[ad] Reed W Smith,[ab] Tor Svensson,[ab] Ina Terstiege,[ab] Christian Tyrchan,[ab] Wenzhen Yang,[f] Shuchun Zhao,[f] Linda Öster.[e] .*

[a] Respiratory, Inflammation and Autoimmunity, Innovative Medicines and Early Development, AstraZeneca Gothenburg, Pepparedsleden 1, SE-431 83 Mölndal, Sweden, [b] Medicinal Chemistry, [c] DMPK, [d] BioScience, and [e] Discovery Sciences, Innovative Medicines and Early Development, AstraZeneca Gothenburg, Pepparedsleden 1, SE-431 83 Mölndal, Sweden, [f] Pharmaron Beijing Co., Ltd., No.6 Taihe Road, BDA, Beijing, 100176, P.R. China

ABSTRACT PI3Kδ is a lipid kinase that is believed to be important in the migration and activation of cells of the immune system. Inhibition is hypothesised to provide a powerful yet selective immunomodulatory effect that may be beneficial for the treatment of conditions such as asthma or rheumatoid arthritis. In this work we describe the identification of inhibitors based on a thiazolopyridone core structure and their subsequent optimisation for inhalation. The initially identified compound (**13**) had good potency and isoform selectivity

but was not suitable for inhalation. Addition of basic substituents to a region of the molecule pointing to solvent was tolerated (enzyme inhibition pIC_{50} >9) and by careful manipulation of the pKa and lipophilicity we were able to discover compounds (**20b**, **20f**) with good lung retention and cell potency that could be taken forward to *in-vivo* studies where significant target engagement could be demonstrated.

Introduction

Phosphoinositide 3-kinases (PI3Ks) are a group of enzymes that are involved in the phosphorylation of the membrane-bound inositol phospholipids in the 3-position of the inositol moiety. The eight known members are divided into three classes, I, II and III. Class I PI3Ks have been the most extensively studied of these subclasses; the class is further subdivided into IA (PI3Kα, β & δ) and class IB (PI3Kγ) based upon the types of regulatory subunits with which the catalytic domains combine in the active heterodimeric forms. Class 1A PI3Ks mediate the signal transduction from receptor tyrosine kinases whilst PI3Kγ is principally activated by GPCRs. PI3Kδ & γ are restricted to cells of the haematopoietic system whilst PI3Kα & β are ubiquitous. Dysregulation of the PI3K system (the kinases and the associated phosphatases) is often observed in cancers and there has been a great deal of interest in developing pan or selective inhibitors of PI3Ks for applications in oncology.[1,2] Evidence is growing that inhibition of PI3Kδ and/or γ can have powerful yet selective effects on the immune response and inhibitors have attracted interest as potential treatments for diseases with a significant immunological component, such as rheumatoid arthritis and asthma.[3-6] Understanding of the biology of PI3Ks is developing fast, however there are still details and subtleties to be worked out. Several reviews describe the current state of knowledge.[7-10,]

Recently the PI3Kδ selective inhibitor idelalisib (Figure 1, **A**) has been launched as the first PI3K inhibitor to market for the treatment of B-cell cancers.[11] The drug is effective but shows a number of significant side-effects.[12]

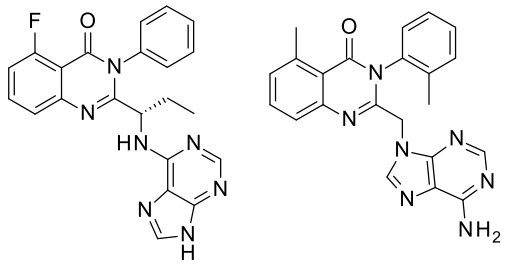

Figure 1. Reference PI3Kδ inhibitors.

We were interested in PI3Kδ as a potential treatment for lung conditions such as asthma. We have previously described an earlier series of PI3Kδ inhibitors that we investigated but which showed disappointing cell potencies.[13] We selected an inhaled approach with a view to minimising the systemic exposure and thus the potential for side-effects from either target-related or off-target interactions. This early decision to follow an inhaled approach mandated several aspects of our medicinal chemistry strategy: i, The limitations on dose deliverable through standard inhalers meant that achieving sub-nanomolar potency was crucial. ii, Soluble compounds are typically cleared from the lungs in a matter of minutes[14] whilst inflammatory cells are recruited to the lung continuously, so sufficient exposure and retention in the lung is required. iii, In order to minimise systemic exposure oral bioavailability should be low and plasma clearance high.

Multiple chemotypes have been described as PI3Kδ selective inhibitors.[15] Broadly speaking they fall into two categories, "propeller" shaped compounds, such as idelalisib, that access an induced pocket[16] and other chemotypes that all appear to derive selectivity by a

combination of optimising the interactions in the affinity pocket for PI3Kδ and accessing the "tryptophan shelf". The "tryptophan shelf" describes the face of Tyr760 (PI3Kδ numbering) which is accessible in PI3Kδ owing to the small size of Thr750, whereas larger residues in the corresponding positions of PI3Kα, β and γ occlude this surface.[17]

Since the disclosure of the structure of IC87114[18] (Figure 1, **B)** in 2003 there has been extensive medicinal chemistry exploration of chemotypes that can give "propeller" type structures.[15] We started our search for PI3Kδ inhibitors by looking for a novel propeller-shaped chemotype in view of the heavy patenting around 6,6-fused systems such as isoquinolinones and quinazolinones. We identified the thiazolopyridone ring system as a potentially suitable core for our explorations. Since the completion of the work described herein but prior to the submission of this article the same core has been described in the patent literature for some PI3Kδ inhibitors.[19]

Chemistry

Synthesis of the compounds described in this paper followed a general route with late-stage diversification in order to introduce changes to the aryl substituents. The route (Scheme **1)** started by following the procedures described by the Almqvist group for the synthesis of 6-bromothiazolidinopyridones.[20,21] Initially we used a racemic synthesis with late-stage chiral separation but the majority of work was carried out starting with chiral (R)-2-chloropropionic acid. Coupling of this acid with Meldrum's acid gave dioxinone **3**. This dioxinone reacted thermally with thiazoline **2** to give the core ring system **4** as a mixture of diastereomers. Ring bromination of **4** was followed by sulfoxidation, Pummerer rearrangement and elimination to deliver the aromatised compound **7**. Displacement of the chlorine with sodium azide followed by reduction gave amine **9**. CBZ protection of the free amine produced carbamate **10.**

Suzuki coupling of racemic **10** from the initial synthesis with phenyl boronic acid gave **11** that was deprotected to amine **12** which on heating with 4-amino-6-chloropyrimidine-5-carbonitrile, followed by separation of the enantiomers by chiral HPLC produced initial lead **13** (Scheme **2**).

Chiral analysis of **10** produced using (R)-2-chloropropionic acid showed that some loss of stereochemical purity had occurred during the synthesis. **10** however proved to be suitable for chiral SFC and could be purified to >99% enantiopurity. Cleavage of the carbamate returned chirally pure amine **9** that was used as the starting point for subsequent exploration (Scheme **3**). Heating amine **9** and 4-amino-6-chloropyrimidine-5-carbonitrile in n-butanol gave the bromide **14** that was coupled with substituted phenyl boronic acids to give, after deprotections and, where required, reductive amination, compounds **15a** and **17-19**. Alternatively use of an aldehyde functionalised boronic acid gave intermediate **16** that could be reductively aminated with a range of amines to give, in some cases after additional manipulation, compounds **15b-g** and **20a-l**.

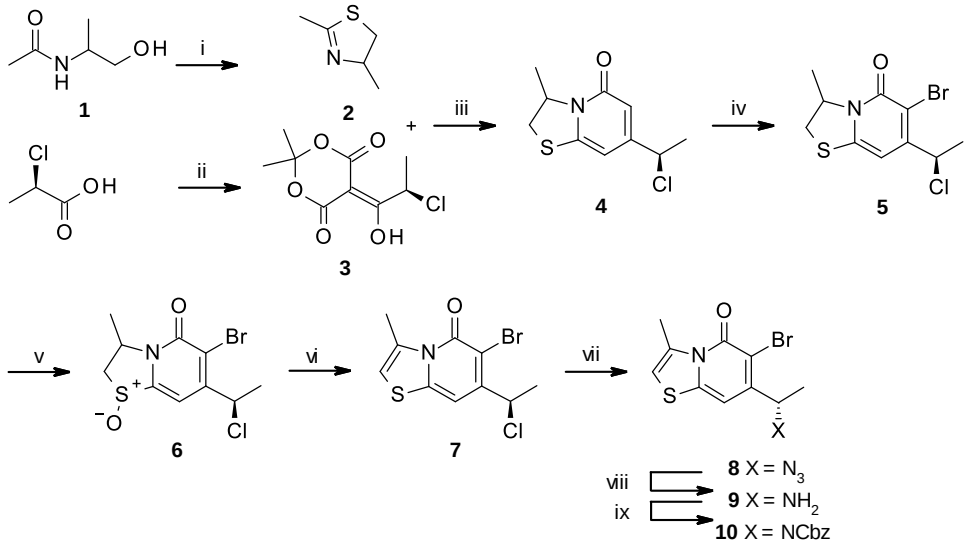

Scheme 1.

i, Lawesson's reagent, THF, 65 ºC ii, Meldrum's acid, DCC, DMAP, CH_2Cl_2 iii, TFA, TFAA, $ClCH_2CH_2Cl$ iv, isoamyl nitrite, HBr (40% aq), CH_2Cl_2, <-5 °C v, mCPBA, CH_2Cl_2, 0 °C vi, TFAA, PhMe, 60 °C then cH_2SO_4, CH_2Cl_2, 0 °C - RT vii, NaN_3, DMF, 45 ºC viii, Ph_3P, CH_2Cl_2, reflux ix, CbzCl, K_2CO_3, THF: water 10:1, 0 °C

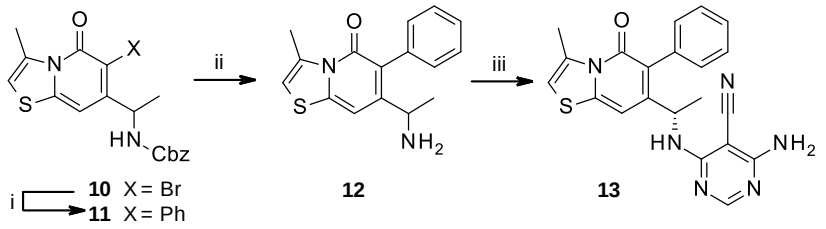

Scheme 2.

i $PhB(OH)_2$, $PdCl_2(dppf).CH_2Cl_2$, DME-water , 100 ºC ii, BBr_3, CH_2Cl_2, 0 °C - RT iii, 4-amino-6-chloropyrimidine-5-carbonitrile , DIEA, n-butanol, 120 ºC then Chiral HPLC

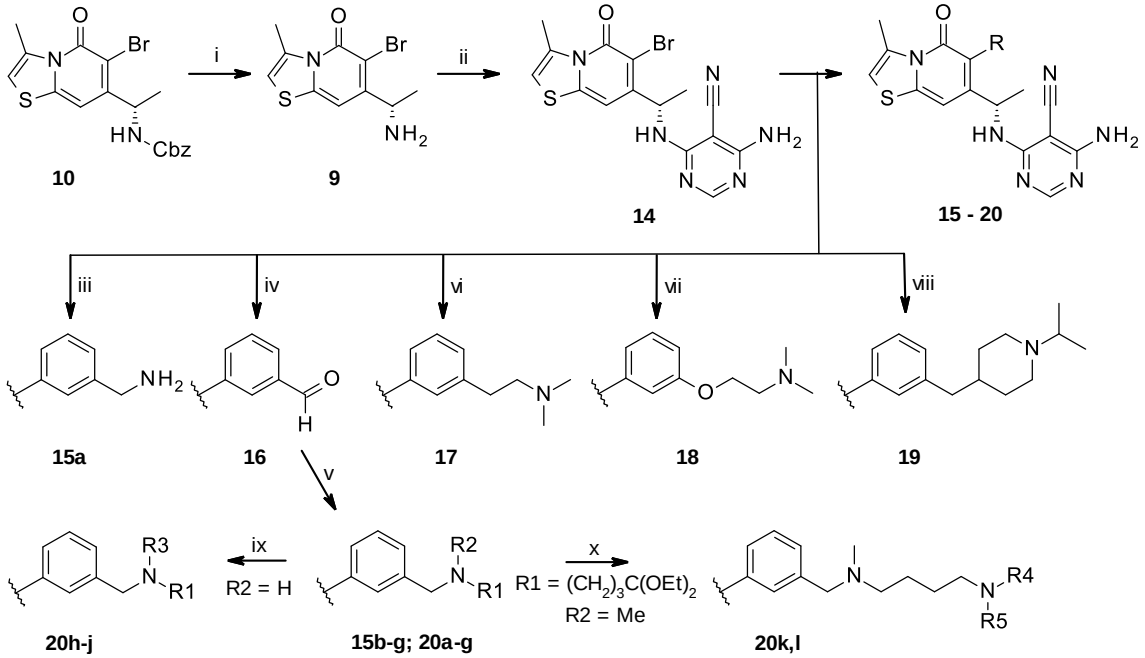

Scheme 3.

i, BBr_3, CH_2Cl_2, 0 °C - RT ii, 4-amino-6-chloropyrimidine-5-carbonitrile , DIEA, n-butanol, 120 °C iii, $ArB(OH)_2$, $PdCl_2(dppf).CH_2Cl_2$, Cs_2CO_3, DME-water, 100 ºC then TFA, CH_2Cl_2 iv, $ArB(OH)_2$ $PdCl_2(dppf).CH_2Cl_2$, Cs_2CO_3, DME-water, 100 ºC v HNRR, $NaBH_3CN$, MeOH-CH_2Cl_2 vi, a) $ArB(pinacol)$, 3rd generation Pd precatalyst, $P(Cy)_3.HBF_4$, K_3PO_4, dioxan-water, 130 °C b) TFA, CH_2Cl_2 c) CH_2O, $NaBH_3CN$, AcOH, MeOH vii, $ArB(pinacol)$, 3rd generation Pd precatalyst, $P(Cy)_3.HBF_4$, K_3PO_4, dioxan-water, 130 ºC then

DEAD, $Me_2NCH_2CH_2OH$, Ph_3P, THF, 0 ºC viii, a) ArB(pinacol), Pd dppf, Cs_2CO_3, dioxan-water, 130 ºC b) TFA, CH_2Cl_2 c) acetone, $NaBH_3CN$, AcOH, CH_2Cl_2-MeOH ix, $NaBH_3CN$, acetaldehyde or CH_2O, AcOH, CH_2Cl_2-MeOH x, a) CH_2O, $NaBH_3CN$, AcOH, MeOH b) TFA / CH_2Cl_2-water c) amine, $NaBH_3CN$, AcOH, CH_2Cl_2-MeOH

Results and discussion

Initial thiazolopyridone **13** met our criteria for a lead with excellent PI3Kδ potency in both biochemical and cellular assays, very good selectivity against PI3Kα and acceptable selectivity against PI3Kβ and γ (Table 1).

Table 1. SAR of *m*-benzylamines.

Compound	R	PI3K pIC_{50}					Solubility μM	LogD
		δ	α	β	γ	δ cell		
13	H	9.4	6.2	7.3	7.9	9.2	77	2.7
15a	CH_2NH_2	9.2	5.9	8.1	6.7	7.4	>1000	-0.3
15b	CH_2NHMe	9.1	5.9	8.0	6.2	7.7	>1000	-0.2
15c	CH_2NMe_2	9.1	5.5	7.2	6.2	8.8	956	0.8
15d	$CH_2NHCH_2CH_2OMe$	9.2	5.9	7.7	6.4	8.6	>1000	0.7
15e	$CH_2N(Me)CH_2CH(Me)_2$	9.3	5.7	7.0	<6.1	9.2	12	2.3
15f	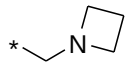	9.3	5.8	7.4	6.3	8.6	954	0.5
15g	$CH_2NH(CH_2)_4O(CH_2)_2Ph$	9.4	6.3	8.1	6.5	8.9	699	2.3

All biological values are mean of ≥ 3 replicates

As a model for inhalation we dosed compounds by intra tracheal (i.t.) administration of a solution of compound to rats followed by termination at time-points up to 24 h and subsequent analysis of the residual compound in the lungs. Compound **13**, a moderately

soluble (77 μM) neutral molecule, was cleared extremely rapidly from lung; compound could only be detected at the first time-point (3 minutes after dosing, table **2**). Given the rapid clearance from the lung of the parent compound we needed to find a mechanism by which we could obtain duration. Two main strategies have been described to produce a prolonged effect in lung tissue: low solubility[22,23] or basicity.[24] Solubility-driven approaches require that material dissolves slowly over the time after dosing to produce the effect whilst a pH-driven approach relies on dissolved compound being trapped in acidic organelles, such as lysosomes, which are prevalent in lung tissue, to provide a depot that is then released slowly over an extended period of time. We prioritised the addition of basic centres as a potentially predictable method to modulate lung retention.

Crystallisation of **13** in a murine PI3Kδ construct (Figure **2**) showed that the compound bound in a similar conformation and into the same induced pocket in the enzyme that has been described previously.[16] Examination of the crystal structure revealed that there might be scope to extend from the *meta* position of the phenyl ring towards solvent if the phenyl ring made a small rotation, enabling modulation of the physical properties of the compounds without affecting the enzyme affinity.

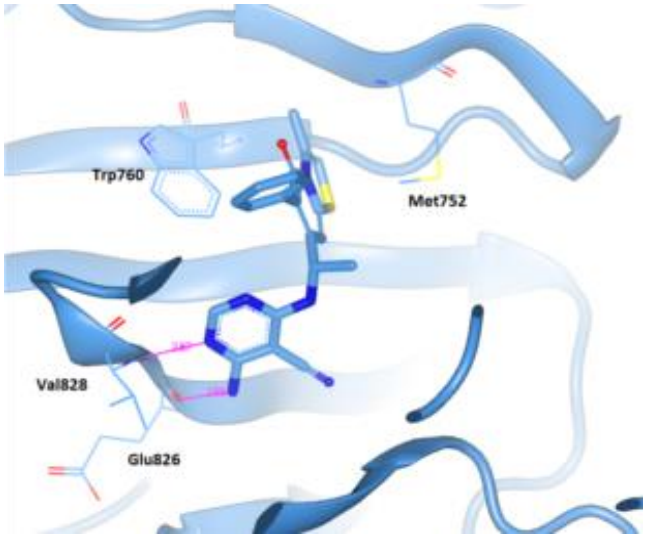

Figure 2. Compound **13** bound in murine PI3Kd showing the ATP binding pocket with the induced pocket between Trp760 and Met752 and with hydrogen bonds to the NH of Val828 and the carbonyl of Glu826 making the hinge interaction.

Table 2. Lung PK of compounds **13**, **15a-g**.

Compound	Lung t½ h	Residual dose at 4 h (%)	Residual dose at 24 h (%)
13	NA*	0	0
15a	1.6	2	0
15b	4.9	2.5	0
15c	2.3	0.2	0
15d	1.3	0.8	0
15e	NA*	0	0
15f	1.1	0.5	0
15g	3.5	4.8	0

All time-points were a mean from 3 animals

* Compounds **13 & 15e** were only detected in lung tissue at the first time-point of the experiment (3 minutes after dosing) and then only 2 % and 6.5 % of the total dose respectively.

Addition of a benzylic amine to the meta position of the pendant phenyl in **13** gave compounds (**15a**, **b**, **c**) that retained the PI3Kδ potency of **13** but exhibited differing selectivities towards the other isoforms. (Table 1) Addition of the basic centre increased selectivity towards PI3Kγ by reducing potency at that isoform, particularly for **15b** & **c**, thus increasing selectivity. Selectivity towards PI3Kβ on the other hand was reduced for **15a** & **b**, though not for **15c**. Selectivity against PI3Kα was slightly increased, with **15c** again the most selective. All three compounds had low lipophilicity, particularly **15a** & **b**, and these two

showed a significant potency drop-off in the cell assay, probably reflecting poor cell permeability.

Crystallisation of **15c** with PI3Kδ (Figure **3**) showed an almost complete superposition with the structure of **13** without rotation of the phenyl ring; the dimethylamino group, as expected, pointed into the solvent channel. The dimethylamino group lies in the proximity of Asn836 (PI3Kδ), the amide moiety of which can be seen to rotate slightly to accommodate the ligand; this is one of the few highly variable residues in the vicinity of the ATP binding site of the highly homologous PI3K isoforms. The corresponding residues in the other isoforms PI3Kα Gln859, PI3Kβ Asp856 and PI3Kγ Lys890 are all different. These differences can in part explain the observed selectivity changes, thus the positively charged protonated amines can make a favourable interaction with the aspartate anion of PI3Kβ that is reflected in the increased potency at this isoform, but make an unfavourable one with the cation of Lys890 in PI3Kγ accounting for the big drop in potency observed. The neutral glutamine in PI3Kα has a more modest effect, but is a larger group than the asparagine in δ and thus the slight loss of potency as the size of the substituent increases from **15a** to **b** to **c** can be understood. These effects were seen consistently for further examples (**15d**–**f**) and consequently we shifted our focus to tertiary amines in this position to ensure we obtained sufficient selectivity vs. PI3Kβ.

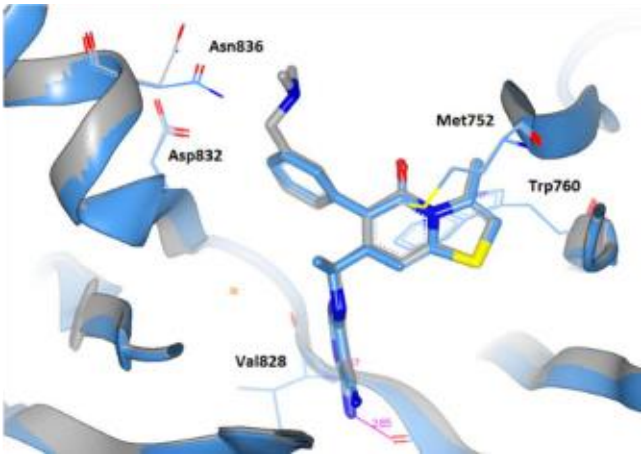

Figure 3. View of **15c** (grey) overlayed with **13** (blue) showing the very similar conformations adopted by the ligands and the almost identical protein conformations. Note the movement of the sidechain amide of Asn836 permitting the dimethylamino group to be accommodated.

Larger N-substituents were tolerated, as expected based on this group pointing to solvent (Figure **4**), and enzyme affinities at all four isoforms were remarkably consistent across the series **15a-g**, barring the effect already mentioned with PI3Kβ. More lipophilic compounds however showed improved cell potencies, consistent with a potential favourable effect on membrane permeability (Table **1**, Figure **5).** We investigated the preferred location of the basic centre by making a series of changes to the linker length between the amine and the aromatic ring (**17**, **18**, **19**, Table **3**). As the distance between the amine and the aromatic ring increased beyond two atoms the potency at PI3Kβ reduced, consistent with loss of a favourable interaction with Asp856; activity against the other isoforms was little changed. Once again cell potency dropped off for compounds with low LogD.

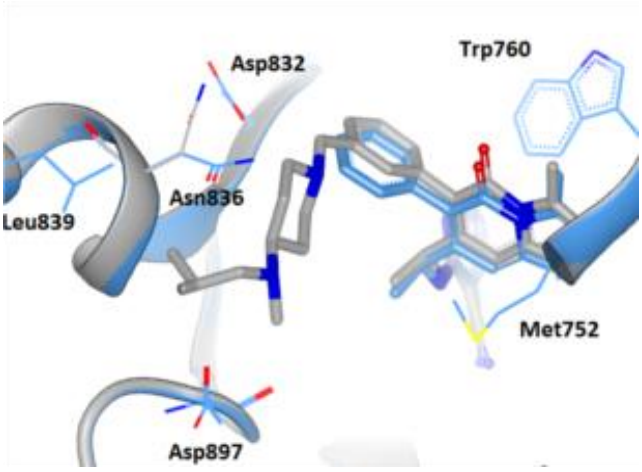

Figure 4. Docked structure of **20f** (grey) overlaid with **13** (blue) in murine PI3K showing the large substituted aminopiperidine accommodated in the solvent channel.

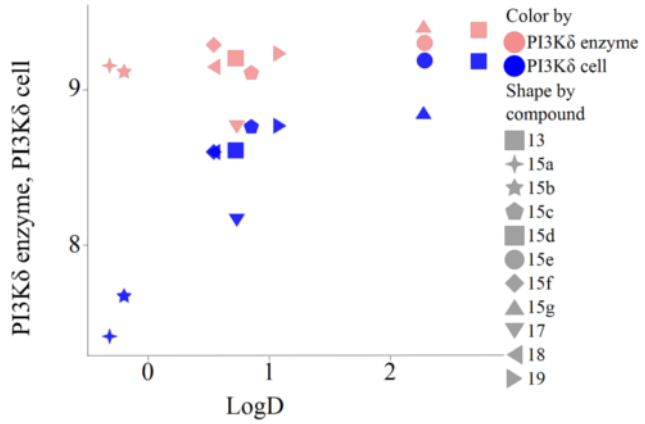

Figure 5. Enzyme and cell potencies for compounds **13**, **15a-g**, **17**, **18**, **19** showing cell drop-off at low lipophilicity.

Table 3. SAR of alternate positions for the base.

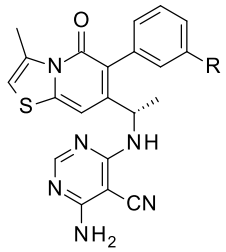

15c, 17-19

Compound	R	PI3Kδ pIC_{50}	PI3Kα pIC_{50}	PI3Kβ pIC_{50}	PI3Kγ pIC_{50}	PI3Kδ cell pIC_{50}	Log D
15c	CH_2NMe_2	9.1	5.5	7.2	6.2	8.8	0.8
17	$CH_2CH_2NMe_2$	9.1†	5.9†	7.3†	<6.0†	8.6‡	0.5
18	$OCH_2CH_2NMe_2$	8.8	5.1	6.7	6.5	8.2	0.7
19	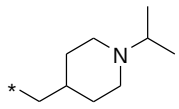	9.2	6.0	6.4	6.6	8.8	1.1

All biological values are means of ≥ 3 replicates except † n= 1and ‡ n = 2

In contrast to compound **13**, i.t. dosing of **15a**-**g** to rat lung showed measureable half-lives for all except **15e**, but the vast majority of compound was still cleared within a short period and negligible compound was present 24 h after dosing for any of the compounds. (Table **2**) We focussed on the amount of compound retained at 4 and 24 h to guide our design rather than the half-life as the latter reflected the terminal β-phase only and did not account for differences in the amount of compound lost in the rapid initial α-phase, which was often >99% (Figure **5**). Compounds **15e** and **g** both met the criteria of Austin et al[25] for obtaining duration with inhaled β-agonists (pKa > 8, LogD > 2; pKa could not be determined for **15e** but related tertiary benzylamines had pKa > 9; pKa **15g** = 9.4). The long phenylethoxyalkyl chain of **15g** was modelled on that used for β-agonists like Salmeterol and Sibenadet.[26] Despite these precedents **15e** was barely retained at all in lung whilst **15g**, though having the greatest retention of this group of compounds, still exhibited insufficient lung residence for our purposes.

In parallel with our investigations of basic sidechains we sought to investigate dibasic analogues. (Table **4**) The first two compounds synthesised (**20a**, **b**) were highly potent PI3Kδ inhibitors. As with the monobases the secondary amine **20a** was less selective against PI3Kβ then the tertiary amine **20b**. Both compounds showed reduced cell potency, consistent with their low lipophilicities. When dosed IT to rats **20b**, but not **20a**, showed excellent lung retention with both a long half-life and a substantial proportion of the dose remaining in the lung 24 h after dosing (table **4,** Figure **6**). For **20b** there was still an initial α-phase with a rapid decrease of compound over the first 30 minutes, followed by a prolonged β-phase where the levels declined slowly however dibase **20b** exhibited the base-driven PK profile that we were seeking for our compounds.

Table 4. Data for dibasic compounds **20a-l**.

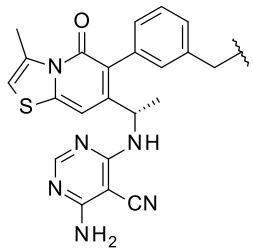

20a-l

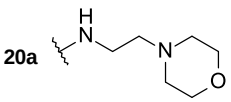

20a

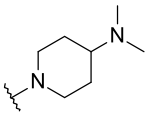

20b

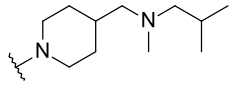

20c

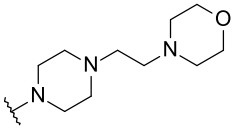

20d

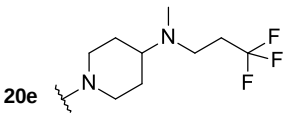

20e

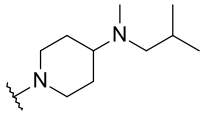

20f

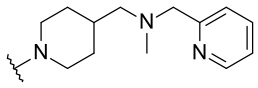

20g

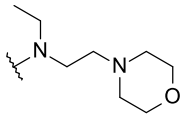

20h

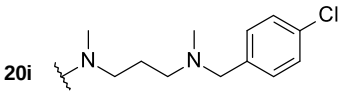

20i

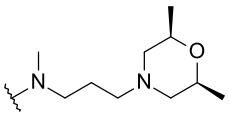

20j

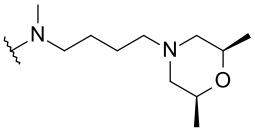

20k

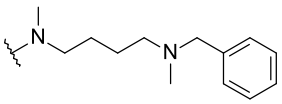

20l

Compound	PI3Kδ pIC_{50}	PI3Kβ pIC_{50}	PI3Kδ cell pIC_{50}	LogD	ClogP	pKa B1	pKa B2	Lung t½ h	Residual dose at 24 h (%)
20a	9.2	7.7	7.9	0.6	2.7	9.6	4.7	4.2	0.1
20b	9.3	7.2	8.0	0.5	2.7	9.5	6.5	23.2	4.8
20c	9.2	7.3	8.6	2.1	4.8	9.8	8.0	12	3.3
20d	9.1	7.0	9.0	2.5	3.5	8.4	5.4	4.5	0.2
20e	8.8	6.6	7.9	1.1	2.6	7.3	6.0	8.7	3.5
20f	9.2	7.1	8.9	1.7	4.2	9.7	6.8	9.9	2.8
20g	9.1	7.2	8.7	2.0	3.8	9.0	7.0	10.9	5.2
20h	9.1	6.6	8.9	1.4	3.8	8.0	4.0	0.0	0.0
20i	9.2	7.9	8.5	3.2	6.1	8.8	7.5	13	3.3
20j	8.9	6.9	8.3	1.5	4.4	8.5	5.7	5.9	0.8
20k	8.9	7.1	8.2	1.5	4.3	8.9	6.3	7.6	3.9
20l	9.3	7.8	8.7	2.2	5.1	9.1	7.0	17.6	7.4

pIC_{50} values for PI3Kα and γ not shown; these were consistently low (α ≤ 6.2, γ ≤ 6.7) All biological values are means of ≥ 3 replicates

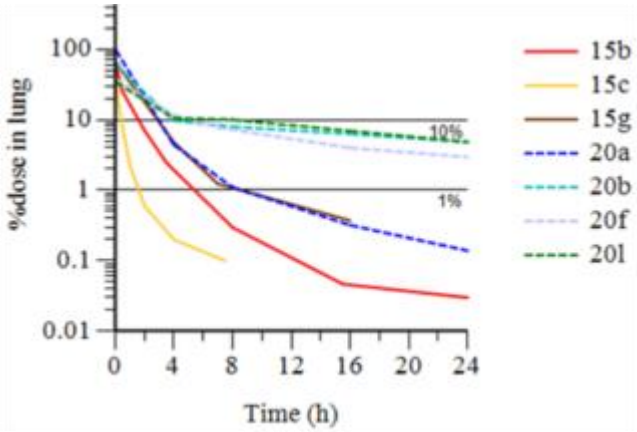

Figure 6. Rat ITPK time-course profiles of selected examples.

This left the question of why **20b** but not **20a** was retained in lung? Previous work[16] has described the benefits of dibases for lung retention, but the precise basicities required have not been defined. Measured pKas for the two compounds were surprisingly different, with the second pKa for **20b** being markedly higher than that of **20a** (6.5 vs. 4.7). To investigate this effect further we synthesised a set of compounds with a range of pKas for both basic centres (Table **4**). Inevitably these compounds (**20c** - **l**) also had varying lipophilicities; thus we also investigated the role of lipophilicity on both cell potency and PK. (Figures **7** & **8)**

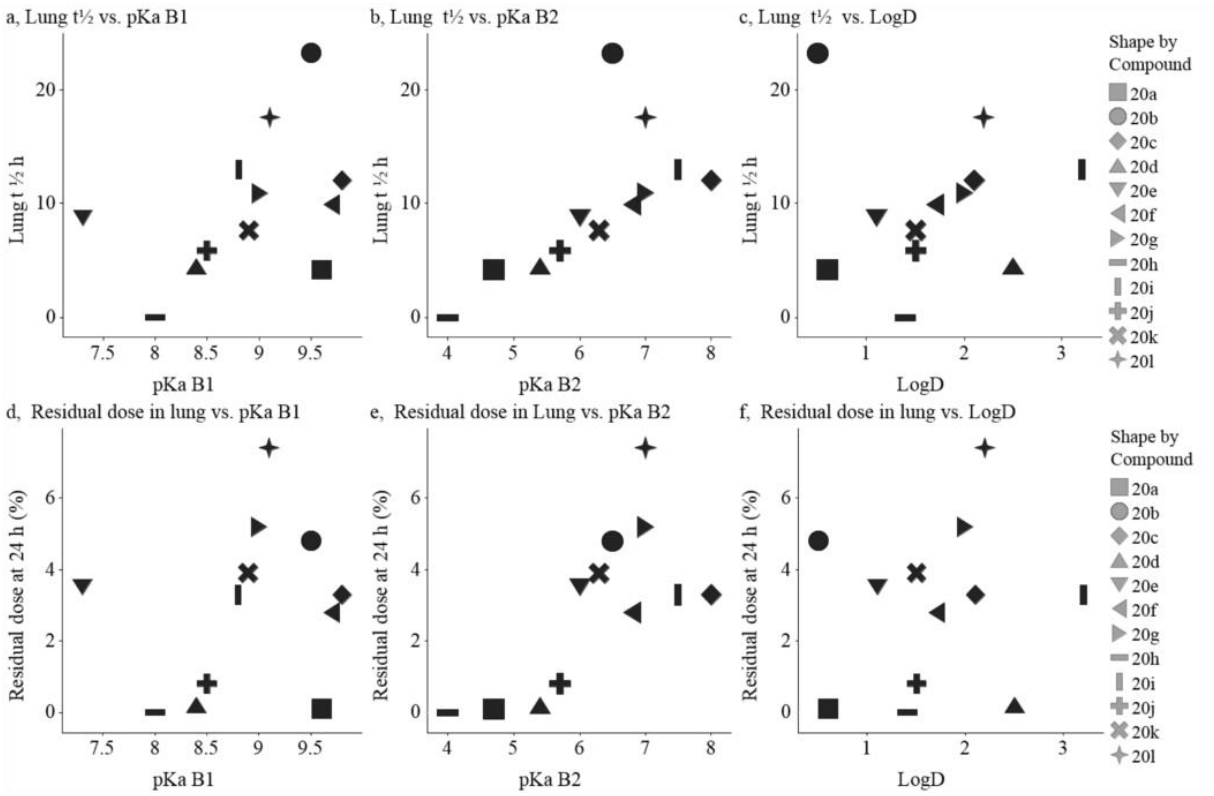

Figure 7. Relationships between lung retention (% remaining at 24 h; half-life) and the first and second pKas or Lipophilicity (LogD) for dibases

Examination of Figure **7** shows that, for the range of variables tested, the second (weaker) basic pKa is the most significant factor (**6b** & **e**). Thus for compounds with a second pKa less than 5 (**20a**, **20h**) half-life is short (< 4 h) and essentially no compound is retained in the lung at 24 h. As the second pKa is increased the half-life increases but until the second pKa reaches >~6 only a small fraction is retained in the lung after 24 h. With a low second pKa changes in lipophilicity have little effect (**20a** vs. **20h**; **20d** vs. **20j)**. For compounds where the second pKa is greater than 6 further increases provide, in general, an increased lung half-life, but the effect on the absolute retention is less well defined. The first pKa (**6a** & **d)** appears not to play a significant role in the retention of compounds in the lung over the range of values in this series of compounds (lowest pKa B1 7.2). Lipophilicity, as determined by LogD (also similarly for CLogP, data not shown) does not appear to affect the amount of dose

remaining after 24 h (**6f**), but does appear to contribute in a small way to the lung half-life (**6c**).

There are two significant outliers to the analysis described above, compounds **20b** & **20l**. For both of these compounds the half-life is surprisingly long; **20l** also has the highest percentage of sample remaining in the lung after 24 h. **20l** was designed to contain an aralkyl chain similar to that used to improve retention in β-agonists,[26] however the structurally related compound **20i** does not exhibit any marked effect on retention. (Both **20i** and **20l** surprisingly showed a decreased selectivity towards PI3Kβ which ruled out **20l** from further progression despite the excellent lung retention.)

We rationalise these results as implying that lung retention is driven by trapping of a dication in lung lysosomes (pH 4.5 – 5[27]). The monocation is membrane permeable and the rate of escape from the lysosome and hence half-life is driven by the fraction of monocation, affected by the second pKa, and lipophilicity. The effect of lipophilicity on half-life probably principally derives from the greater membrane affinity of the more lipophilic compounds, thus the longest half-life belongs to the least lipophilic dibase **20b**. Additional structural features, like the long aralkyl chain of **20l**, also affect the rate of membrane permeability.

The most important driver of cell-potency appears to be the lipophilicity (Table **4**, Figure **8**). (Compounds where the second pKa is less than 6 are excluded from this analysis as they behave more like monobases.) If LogD is greater than approximately 1.6 then a compound with good enzyme inhibition will also have good cell potency. When a larger and more diverse set of dibases were examined (data not shown) the same trend was still apparent, with a lower cut-off of LogD *ca* 1.4 and an upper cut-off of *ca* 2.8, though structural variations did have an additional effect.

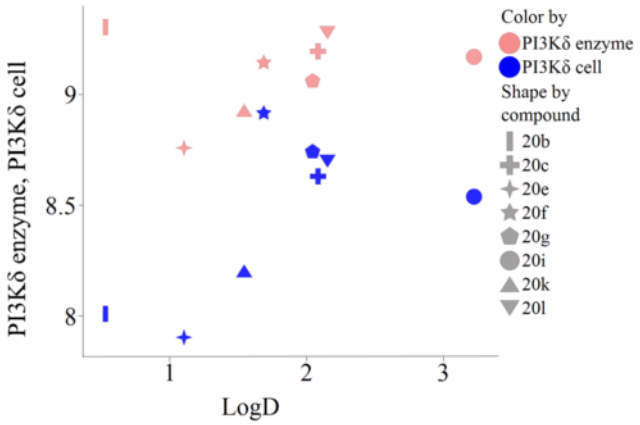

Figure 8. Cell drop-off for dibases.

Compounds **20b** & **f** were selected for further study based on their good lung retention, high potency coupled with isoform selectivity and, for **20f**, excellent cell potency. Both of these compounds were screened against a panel of 345 kinases, neither showed >50% activity at any other kinase at 1 μM. Neither compound showed significant inhibition of the hERG ion channel, despite containing basic centres (< 20 % inhibition at 11 μM).

Dosing to rats both IV and PO (table **5**) showed that the compounds had negligible oral bioavailability and high systemic clearance with **20f** exhibiting clearance greater than liver blood flow, implying that extrahepatic mechanisms were involved. These results gave us confidence that systemic exposure of these two compounds when dosed by inhalation would be low.

Table 5 Rat Pharmacokinetics IV and PO.

Example	IV Clearance mL/min/kg	t ½ h	Vss L/kg	Oral bioavailability %
20b	57	12	12	<1
20f	150	11	88	<1

All values determined from 2 animals

To study the effects of the compounds in an inhaled setting we used a transgenic mouse model as a mechanistic model of T-cell activation. Briefly transgenic mice (OTII strain, genetically sensitised to ovalbumin[28]) were challenged with ovalbumin (dosed i.t.) and then, after a week, dosed with compound (i.t. administration) 2h prior to a challenge with intranasal anti-CD3. The animals were terminated 6 h after challenge and the inhibition of the formation of phospho S6 ribosomal protein (pS6RP) by compound was determined as a biomarker for the inhibition of PI3Kδ.[29] **20b** showed good activity in this model with a clear dose response, although a high dose was required to achieve full effect (Figure **9a**). When **20f** was dosed similarly a significant effect was observed, however instead of the 10-fold improvement in efficacy that we were hoping to see, based on the significantly better cell potency of this compound, the effect appeared to be weaker. (Figure **9b**).

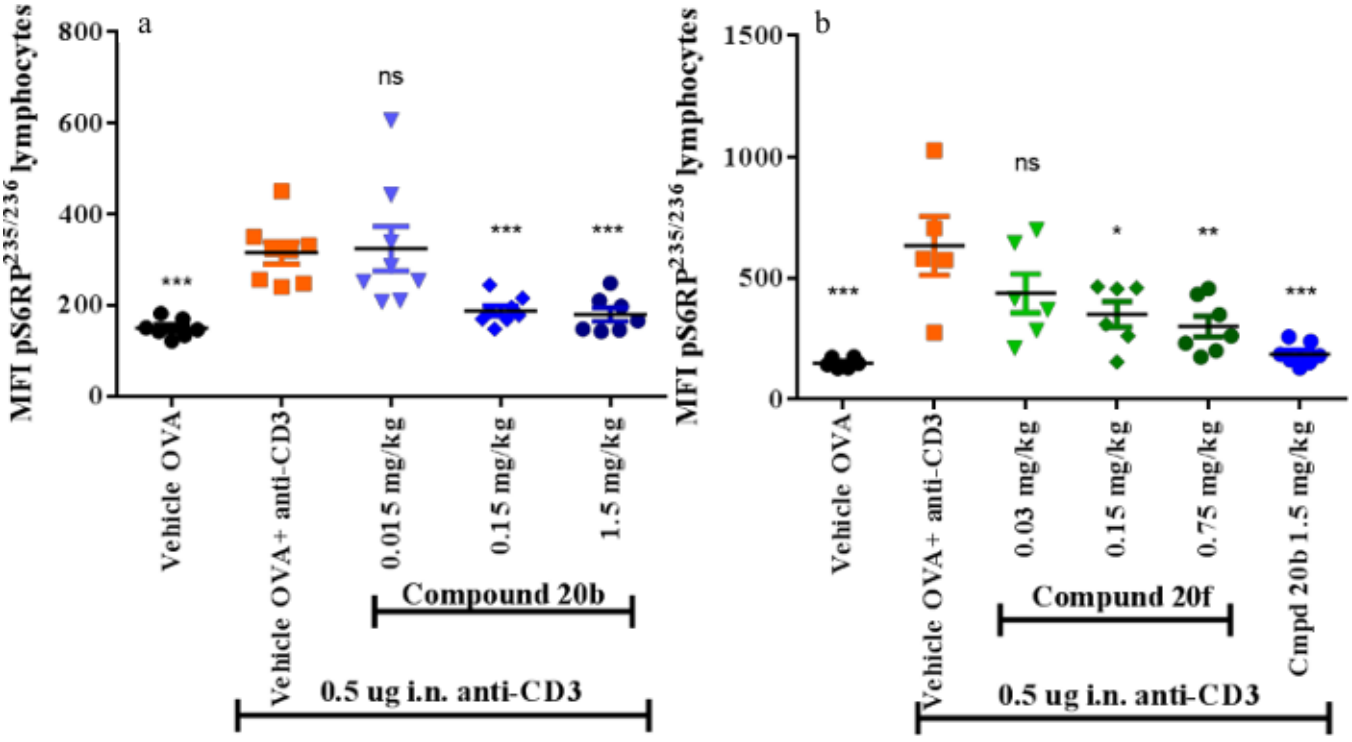

Figure 9. Inhibition of pS6RP in lung lavage after anti-CD3 challenge to OTII mice. **9a** compound **20b** **9b** compound **20f.** Target engagement of PI3Kδ activity is shown through

measurements of pS6RP in bronchoalveolar lung lavage cells after anti-CD3 challenge to OVA-challenged OTII mice. Phosphorylation of S6RP, measured using phosphospecific antibodies, was significantly inhibited by both **20b** (9a) and **20f** (9b) in a dose-dependent manner, however the inhibition by **20b** showed better potency. Data is shown as results for individual animals at each dose with the statistical significance indicated as follows above the columns : p<0,001 ***; p<0,005 **; p<0,05 *

This result left us with the question of why the more potent compound *in vitro* appeared to be less effective *in-vivo*? Our rationalisation is that although **20f** is retained in the lung effectively we do not know the available levels of drug at the target in the lung. Compound in the lung is expected to be partitioned between acidic organelles, membranes and lung fluid. Different ratios in this partitioning will produce differing concentrations of free drug available to act on the T-cells that drive the observed results. It is also believed that, for highly permeable compounds such as this series, free drug in lung partitions rapidly into the systemic circulation. Given the very high systemic clearance of these compounds it is unlikely that an equilibrium can be achieved and instead that free drug in the lung will continually be lost to the systemic circulation, resulting in very low lung free levels, once the initial dose has distributed. Based on this analysis we concluded that unfortunately the combination of a lipophilic dibasic molecule with the very high systemic clearance exhibited by this series was unlikely to deliver a compound with sufficient *in-vivo* potency to be capable of being administered at the low dose necessitated by inhaled delivery and that we would require a different chemical series with alternative properties to deliver the effect that we desired.

Conclusions

We have identified a novel scaffold with excellent potency against PI3Kδ and good selectivity against the other isoforms, particularly PI3Kα. Guided by crystal structure information we identified a region where we were able to make changes without significantly affecting biochemical potency against

PI3Kδ and were able to identify how to maintain selectivity against PI3Kβ. By exploration of the physical properties of the compounds we were able to identify regions of property space where significant lung retention over 24 h and good cell potency were achievable. From within this property space compounds suitable for further study were identified and we were able to show an effect in a PD model with i.t. dosing.

Chemical Experimental

All reagents obtained from commercial sources were used without further purification; anhydrous solvents were used without further drying. All compounds were purified to ≥95% purity as judged by HPLC with uv and MS analysis. When Cl or Br was present, expected isotopic distribution patterns were observed. Details of the analytical conditions and observed purities are contained in the Supporting Information. Proton (^{1}H) and carbon (^{13}C) NMR spectra were recorded at ambient temperature. Solutions were typically prepared in deuterated dimethyl sulfoxide (DMSO-d_6), deuteromethanol (CD_3OD) or duterochloroform ($CDCl_3$) with chemical shifts referenced to solvent as an internal standard. ^{1}H NMR data are reported indicating the chemical shift (δ), the multiplicity (s, singlet; d, doublet; t, triplet; q, quartet; m, multiplet; br, broad; dd, doublet of doublets; etc.), the coupling constant (J) in Hz, and the integration (e.g., 1H).

5-[(2R)-2-Chloro-1-hydroxypropylidene]-2,2-dimethyl-1,3-dioxane-4,6-dione (3)

A 20 L 4-necked round-bottom flask was charged with (2R)-2-chloropropanoic acid (450 g, 4.15 mol) in dichloromethane (9 L), 2,2-dimethyl-1,3-dioxane-4,6-dione (600 g, 4.16 mol) and 4-dimethylaminopyridine (560 g, 4.58 mol). A solution of DCC (946 g, 4.58 mol) in dichloromethane (2 L) was added dropwise with stirring at 0 ºC. The resulting solution was stirred for 3 h at room temperature, recooled to 0 ºC and was then quenched by the addition of 10 L of 6% $KHSO_4$. The mixture was filtered and the filtrate was extracted with 4 × 15 L of dichloromethane. The combined organic layers were washed with 15 L of brine. The mixture

was dried over sodium sulfate and concentrated under vacuum. The residue was chromatographed (silica gel; PE:EtOAc (10:1)) to give the title compound (460 g, 47%) as a red oil.

^{1}H NMR (300 MHz, $CDCl_3$) δ 1.72 – 1.77 (m, 9H), 6.05 (q, *J* = 6.8 Hz, 1H), 15.58 (s, 1H); m/z (ESI) 232.9 $[M-H]^-$.

7-[(1R)-1-Chloroethyl]-3-methyl-2H,3H,5H-[1,3]thiazolo[3,2-a]pyridin-5-one (4)

A 20 L 4-necked round-bottom flask was charged with 2,4-dimethyl-4,5-dihydro-1,3-thiazole[30] (650 g, 5.64 mol), DCE (6.5 L), trifluoroacetic acid (643 g, 5.64 mol) and TFAA (1185 g, 5.64 mol). The mixture was stirred to get a solution and was heated to 50 ºC. A solution of 5-[(2R)-2-chloro-1-hydroxypropylidene]-2,2-dimethyl-1,3-dioxane-4,6-dione (**3**, 3971 g, 16.92 mol) in DCE (4 L) was added dropwise over 2 h. The resulting solution was stirred overnight at 50 ºC and then allowed to cool to RT. The pH was adjusted to 8 with aq. sodium bicarbonate and the resulting solution was extracted with 3 × 10 L of dichloromethane and the organic layers were combined. The resulting mixture was washed with 1 x 10 L of brine, dried over anhydrous magnesium sulfate, concentrated and chromatographed (silica gel, ethyl acetate/petroleum ether (1:2-1:1)) to give the title compound (668 g, 52%) as a red oil.

^{1}H NMR (400 MHz, $CDCl_3$) δ 1.49 (d, *J* = 6.4 Hz, 3H), 1.71 (d, *J* = 6.8 Hz, 3H), 2.97 (d, *J* = 11.1 Hz, 1H), 3.67 (dd, *J* = 11.1, 7.5 Hz, 1H), 4.73 (q, *J* = 6.8 Hz, 1H), 5.2 – 5.3 (m, 1H), 6.21 (s, 1H), 6.22 (s, 1H)); m/z (ESI) 230/232 (Cl pattern) $[M+H]^+$.

6-Bromo-7-[(1R)-1-chloroethyl]-3-methyl-2H,3H,5H-[1,3]thiazolo[3,2-a]pyridin-5-one (5)

A 10 L 4-necked round-bottom flask was charged with 7-[(1R)-1-chloroethyl]-3-methyl-2H,3H,5H-[1,3]thiazolo[3,2-a]pyridin-5-one (**4**, 312 g, 1.36 mol), dichloromethane (6 L), HBr (40% aq, 288 g, 1.42 mol) and cooled to -10 ºC. 3-Methylbutyl nitrite (318 g, 2.72 mol) was added dropwise with stirring and the resulting solution was stirred overnight at -5 ºC. The

solution was diluted with 3 L of CH_2Cl_2 and was washed sequentially with 2 × 3 L of satd. sodium bicarbonate, 2 × 3 L of 10 % $Na_2S_2O_3$ and 3 L of brine, then dried ($MgSO_4$), filtered and concentrated. The residue was chromatographed (silica gel; ethyl acetate/petroleum ether (1:2)) to give the title compound (295 g, 70%) as a yellow solid.

^{1}H NMR (300 MHz, $CDCl_3$) δ 1.52 (d, J = 6.4 Hz, 3H), 1.70 (d, J = 6.8 Hz, 3H), 3.00 (d, J = 11.2 Hz, 1H), 3.65 – 3.76 (m, 1H), 5.24 – 5.34 (m, 1H), 5.34 – 5.44 (m, 1H), 6.40 (d, J = 2.5 Hz, 1H)); m/z (ESI) 308/310/312 (BrCl pattern) $[M+H]^+$.

6-Bromo-7-[(1R)-1-chloroethyl]-3-methyl-5-oxo-2,3-dihydro-5H-[1,3]thiazolo[3,2-a]pyridin-1-ium-1-olate (6)

A 5 L 4-necked round-bottom flask was charged with 6-bromo-7-[(1R)-1-chloroethyl]-3-methyl-2H,3H,5H-[1,3]thiazolo[3,2-a]pyridin-5-one (**5**, 290 g, 940 mmol) and dichloromethane (3 L). The resulting solution was cooled to 0 °C whereupon m-CPBA (178 g, 1.0 mol) was added in several batches. The resulting solution was stirred for 3 h and was then quenched by the addition of 2 L of sat. $NaHCO_3$. The resulting solution was extracted with 3 × 3 L of dichloromethane and the organic layers were combined, dried ($MgSO_4$) and concentrated. The residue was chromatographed (silica gel; ethyl acetate/petroleum ether (1:1-1:0)) to give the title compound (223 g, 73%) as a yellow solid.

2 diastereomers in ca. 1:1 mixture : ^{1}H NMR (300 MHz, $CDCl_3$) δ 1.75, 1.79 (2 × d, J = 6.8 Hz, 3H), 1.86 (d, J = 6.7 Hz, 3H), 3.14 – 3.35 (m, 2H), 5.37 – 5.53 (m, 2H), 7.16, 7.18 (2 × s, 1H)); m/z (ESI) 324/326/328 (BrCl pattern) $[M+H]^+$.

6-Bromo-7-[(1R)-1-chloroethyl]-3-methyl-5H-[1,3]thiazolo[3,2-a]pyridin-5-one (7)

A 5 L round-bottom flask was charged with 6-bromo-7-[(1R)-1-chloroethyl]-3-methyl-5-oxo-2,3-dihydro-5H-[1,3]thiazolo[3,2-a]pyridin-1-ium-1-olate (**6**, 223 g, 687 mmol), toluene (2.3 L) and trifluoroacetic anhydride (721 g, 3.43 mol). The resulting solution was heated to 60 °C for 3 h, then allowed to cool and concentrated. The residue was dissolved in

dichloromethane (250 mL) which was added dropwise to cooled (0 °C) sulfuric acid (98%, 1.3 L) with stirring. The resulting solution was stirred for 1 h at RT. The reaction was poured onto water/ice and the resulting mixture was extracted with 4 × 1 L of dichloromethane. The organic layers were combined, washed sequentially with 2 × 1 L of sodium bicarbonate and 1 L of brine, dried ($MgSO_4$), concentrated and chromatographed (silica gel; ethyl acetate/petroleum ether (1:5-1:2)) to give the title compound (121 g, 55%) as a yellow solid.

^{1}H NMR (300 MHz, $CDCl_3$) δ 1.76 (d, J = 6.8 Hz, 3H), 2.88 (s, 3H), 5.48 (q, J = 6.7 Hz, 1H), 6.34 – 6.54 (m, 1H), 6.91 (s, 1H)); m/z (ESI) 308 $[M+H]^+$.

7-[(1S)-1-Azidoethyl]-6-bromo-3-methyl-5H-[1,3]thiazolo[3,2-a]pyridin-5-one (8)

A 2 L 4-necked round-bottom flask was charged with 6-bromo-7-[(1R)-1-chloroethyl]-3-methyl-5H-[1,3]thiazolo[3,2-a]pyridin-5-one (**7**, 118 g, 366mmol), N,N-dimethylformamide (1.2 L), TEA (3.88 g, 38 mmol) and NaN_3 (27.5 g, 423 mmol). The resulting solution was stirred for 5 h at 45 °C, allowed to cool to room temperature and poured onto water/ice. The resulting mixture was extracted with 4 × 800 mL of dichloromethane and the organic layers were combined, washed sequentially with 10 × 1 L of 5% NaCl, dried ($MgSO_4$) and filtered to give a yellow solution of the title compound that was used without further purification.

^{1}H NMR (400 MHz, $CDCl_3$) δ 1.51 (d, J = 6.7 Hz, 3H), 2.90 (d, J = 1.2 Hz, 3H), 5.12 (q, J = 6.7 Hz, 1H), 6.47 (d, J = 1.2 Hz, 1H), 6.77 (s, 1H), 7.28 (s, 1H)); m/z (ESI) 315 $[M+H]^+$.

7-[(1S)-1-Aminoethyl]-6-bromo-3-methyl-5H-[1,3]thiazolo[3,2-a]pyridin-5-one (9)

a) From compound 8.

A 5 L 4-necked round-bottom was charged with a solution of 7-[(1S)-1-azidoethyl]-6-bromo-3-methyl-5H-[1,3]thiazolo[3,2-a]pyridin-5-one in dichloromethane (3000 mL, previous step) and triphenylphosphine (87.5 g, 334 mmol). The resulting solution was heated to 50 ºC for 3 h, allowed to cool and concentrated. The residue was dissolved in THF (800 mL) and water (400 mL) and the resulting solution was heated overnight at 50 °C

and then allowed to cool. The mixture was concentrated and the residue was chromatographed (silica gel; methanol/dichloromethane (1:100 to 1:20)) to give the title compound (52 g, 60%) as a yellow solid.

^{1}H-NMR (300MHz, CD_3OD) δ 1.31 (3H, d J = 6.6 Hz), 2.78 (3H, s), 4.40 (1H, q J = 6.6 Hz), 6.84 (1H, s), δ 7.05 (1H, s)); m/z (ESI) 287 $[M+H]^+$.

b) from compound 10

(S)-Benzyl (1-(6-bromo-3-methyl-5-oxo-5H-thiazolo[3,2-a]pyridin-7-yl)ethyl)carbamate (**10**, 10 g, 23.7 mmol) was dissolved in CH_2Cl_2 (200 mL) and cooled to 0°C. Boron tribromide (59.5 g, 237 mmol) was added dropwise over a period of 15 minutes. The resulting mixture was stirred at RT for 3 hours. The reaction mixture was poured onto ice (150 mL) and extracted with CH_2Cl_2 (3 × 100 mL). The aqueous layer was adjusted to pH = 9 with saturated sodium carbonate and was extracted with CH_2Cl_2 (3 × 25 mL). The solvent was removed under reduced pressure and the residue was dried under vacuum to give the title compound (5.50 g, 81 %) as a yellow solid.

^{1}H NMR (500 MHz, DMSO) δ 1.19 (d, J = 6.6 Hz, 3H), 2.00 (s, 2H), 2.71 (s, 3H), 4.23 (q, J = 6.6 Hz, 1H), 7.02 (s, 1H);^{13}C NMR (126 MHz, DMSO) δ 17.99, 22.99, 50.64, 97.30, 97.86, 104.08, 108.93, 137.44, 148.75, 157.18); m/z (ESI) 287 $[M+H]^+$.

Benzyl [(1S)-1-(6-bromo-3-methyl-5-oxo-5H-[1,3]thiazolo[3,2-a]pyridin-7-yl)ethyl]carbamate (10)

A 3 L 4-necked round-bottom flask was charged with 7-[(1S)-1-aminoethyl]-6-bromo-3-methyl-5H-[1,3]thiazolo[3,2-a]pyridin-5-one (**9**, 52 g, 181 mmol) in THF/H_2O (10:1, 1.1 L) and potassium carbonate (62.6 g, 453 mmol) and cooled to 0 °C. Cbz-Cl (46.4 g, 272 mmol) was added dropwise and the resulting mixture was stirred overnight at room temperature. Water (3 L) was added, the solids were collected by filtration, washed with water (5 × 200 mL) and then with THF/Hexane (1:2) (3 × 200 mL). The crude product was purified by

preparative-SFC (CHIRALPAK IC SFC, 5 × 25 cm, 5 µm; mobile phase A CO_2 (50%), B methanol : CH_2Cl_2 = 2:1(0.2% diethylamine)(50%); detection, UV 220 nm) to give the title compound (23.5 g, 31%) as a light yellow solid.

^{1}H NMR (300 MHz, CD_3OD) δ 1.17 (d, J = 7.0 Hz, 3H), 2.80 (s, 3H), 4.58 (s, 1H), 5.04 (s, 2H), 6.83 (s, 1H), 6.94 (s, 1H), 7.11 – 7.51 (m, 5H); m/z (ESI) 421 $[M+H]^+$; α_D -60.5 ° (c = 5.30 g/L CH_2Cl_2, 21-7 ºC); SFC Chiralpak IC-3 5.0 µm; 100 × 4.6 mm; Mobile phase A: CO_2 B:methanol/0.1% diethylamine T_r 1.47 min; e.r 97.7 : 2.3 (minor isomer T_r 1.14 min)

Benzyl (1-(3-methyl-5-oxo-6-phenyl-5H-thiazolo[3,2-a]pyridin-7-yl)ethyl)carbamate (11)

Cs_2CO_3 (1083 mg, 3.32 mmol), phenylboronic acid (152 mg, 1.25 mmol), $PdCl_2$(dppf)-CH_2Cl_2 adduct (68 mg, 0.08 mmol) and (±) benzyl (1-(6-bromo-3-methyl-5-oxo-5H-thiazolo[3,2-a]pyridin-7-yl)ethyl)carbamate (**10**, 350 mg, 0.83 mmol) were slurried in DME (10 mL) and water (2 mL) and heated to 100 ºC for 30 minutes in a microwave. The solvent was evaporated and the crude product was purified by flash chromatography (silica; 80 to 20% petroleum ether in EtOAc) to give the title compound (236 mg, 68 %) as a yellow solid.

^{1}H NMR (300 MHz, CD_3OD) δ 1.17 (d, J = 7.0 Hz, 3H), 2.80 (s, 3H), 4.58 (s, 1H), 5.04 (s, 2H), 6.83 (s, 1H), 6.94 (s, 1H), 7.11 – 7.51 (m, 11H); m/z (ESI) 419 $[M+H]^+$.

7-(1-Aminoethyl)-3-methyl-6-phenyl-5H-thiazolo[3,2-a]pyridin-5-one (12)

To a solution of benzyl N-(1-[3-methyl-5-oxo-6-phenyl-5H-[1,3]thiazolo[3,2-a]pyridin-7-yl]ethyl) carbamate (**11**, 240 mg, 0.57 mmol) in dichloromethane (6 mL) at 0 ºC, was added boron tribromide (863 mg, 3.44 mmol, 6 eq) dropwise. The resulting solution was stirred for 20 h at room temperature and then cooled to 0 ºC. The reaction was quenched by the addition of water/ice, the pH was adjusted to 8 with sodium carbonate (aq.), and the mixture was extracted with chloroform. The organic layers were combined, dried over anhydrous sodium sulfate, and concentrated to give the title compound (120 mg, 74%) as a light yellow solid.

^{1}H NMR (400 MHz, DMSO) δ 1.05 (d, *J* = 6.5 Hz, 3H), 1.93 (s, 2H), 2.68 (s, 3H), 3.68 (q, *J* = 6.6, 1H), 6.91 (s, 1H), 7.09 (s, 1H), 7.20 (d, *J* = 6.0 Hz, 2H), 7.30 (t, *J* = 7.3 Hz, 1H), 7.39 (t, *J* = 7.4, Hz, 2H), 7.50 – 7.67 (m, 1H); m/z (ESI) 285 $[M+H]^+$.

(S)-4-Amino-6-[(1-[3-methyl-5-oxo-6-phenyl-5H-[1,3]thiazolo[3,2-a]pyridin-7-yl]ethyl)amino]pyrimidine-5-carbonitrile (13)

7-(1-Aminoethyl)-3-methyl-6-phenyl-5H-[1,3]thiazolo[3,2-a]pyridin-5-one (**12**, 268 mg, 0.94 mmol) and 4-amino-6-chloropyrimidine-5-carbonitrile[31] (145 mg, 0.94 mmol) were dissolved in n-butanol (12 mL). DIEA (1.21 g, 9.36 mmol) was added and the resulting solution was heated to 120 °C for 2 h, allowed to cool and then concentrated. Recrystallisation (ethyl acetate) gave the title compound (130 mg, 34%) as a light yellow solid. The enantiomers were separated by chiral HPLC (Reprosil NR column 250 × 20 mm eluting with heptane : EtOAc : TEA (40:60:0.1)) collecting the first eluting peak which was then further purified by preparative SFC (Phenomenex Luna Hilic 250 × 30 mm eluting with 20 mM ammonia in methanol) to give the title compound (16 mg).

^{1}H NMR (500 MHz, DMSO-d6) δ 1.23 (d, *J* = 7.1 Hz, 3H), 2.67 (d, *J* = 1.2 Hz, 3H), 4.91 (quint, *J* = 7.0 Hz, 1H), 6.91 – 6.94 (m, 1H), 6.97 (s, 1H), 7.05 – 7.60 (m, 5H), 7.22 (brs, 2H), 7.48 (d, *J* = 7.0 Hz, 1H), 7.95 (s, 1H); ^{13}C NMR (126 MHz, DMSO-d6) δ 18.09, 20.54, 47.72, 67.92, 96.08, 107.52, 115.41, 120.28, 126.76, 127.78 (2C), 130.71 (2C), 136.00, 137.51, 148.16, 152.48, 159.43, 160.88, 161.57, 164.33; m/z (ESI) 403 $[M+H]^+$; HRMS calculated for $C_{21}H_{18}N_6OS$ [(M + H)+], 403.1341; found, 403.1345.

(S)-4-Amino-6-((1-(6-bromo-3-methyl-5-oxo-5H-thiazolo[3,2-a]pyridin-7-yl)ethyl)amino)pyrimidine-5-carbonitrile (14)

(S)-7-(1-Aminoethyl)-6-bromo-3-methyl-5H-thiazolo[3,2-a]pyridin-5-one (**9**, 1.5 g, 5.2 mmol) and 4-amino-6-chloropyrimidine-5-carbonitrile (0.888 g, 5.75 mmol) were dissolved in n-butanol (20 mL). DIEA (9.12 mL, 52.23 mmol) was added and the resulting solution

was stirred at 120 ºC for 12 hours. The solvent was evaporated, the reaction mixture was diluted with EtOAc, and the residual solid was collected to give the title compound (1.50 g, 71 %) as a yellow solid.

^{1}H NMR (500 MHz, DMSO-d6) δ 1.44 (d, *J* = 7.1 Hz, 3H), 2.72 (d, *J* = 1.0 Hz, 3H), 5.38 (quint, *J* = 7.1 Hz, 1H), 6.92 (s, 1H), 7.02 (d, *J* = 1.2 Hz, 1H), 7.28 (brs, 2H), 7.72 (d, *J* = 7.1 Hz, 1H), 7.93 (s, 1H);^{13}C NMR (126 MHz, DMSO-d6) δ 18.0, 19.4, 50.6, 68.3, 96.7, 104.2, 109.1, 115.3, 137.6, 149.0, 153.9, 157.3, 159.6, 161.7, 164.3; m/z (ESI) 405 $[M+H]^+$.[M+H]+ = 405.

(S)-4-Amino-6-((1-(6-(3-(aminomethyl)phenyl)-3-methyl-5-oxo-5H-thiazolo[3,2-a]pyridin-7-yl)ethyl)amino)pyrimidine-5-carbonitrile (15a)

(S)-4-amino-6-((1-(6-bromo-3-methyl-5-oxo-5H-thiazolo[3,2-a]pyridin-7-yl)ethyl)amino)pyrimidine-5-carbonitrile (**14**, 80 mg, 0.20 mmol) was added to a solution of (3-(((tert-butoxycarbonyl)amino)methyl)phenyl)boronic acid (198 mg, 0.79 mmol), cesium carbonate (257 mg, 0.79 mmol) and $PdCl_2$(dppf)-CH_2Cl_2 adduct (16 mg, 0.02 mmol) in DME (2.5 mL) and water (1ml) at 25 ºC over a period of 10 minutes under nitrogen. The reaction was heated to 100 ºC for 45 minutes in a microwave reactor and then cooled to RT. The solvent was evaporated and the residue was purified by flash silica chromatography, elution gradient 60 to 40% petroleum ether in EtOAc to give the (S)-tert-butyl 3-(7-(1-((6-amino-5-cyanopyrimidin-4-yl)amino)ethyl)-3-methyl-5-oxo-5H-thiazolo[3,2-a]pyridin-6-yl)benzylcarbamate (90 mg, 86 %) as a yellow solid.

TFA (2 mL, 25.96 mmol) was added to (S)-tert-butyl 3-(7-(1-((6-amino-5-cyanopyrimidin-4-yl)amino)ethyl)-3-methyl-5-oxo-5H-thiazolo[3,2-a]pyridin-6-yl)benzylcarbamate (80 mg, 0.15 mmol) in CH_2Cl_2 (4 mL) under nitrogen. The resulting solution was stirred at room temperature for 16 hours. The solvent was evaporated and the residue was purified by preparative HPLC with the following conditions: Column: X Bridge C_{18}, 19 × 150 mm, 5 um;

Mobile Phase A:Water/0.05% TFA, Mobile Phase B: MeCN; Flow rate: 20 mL/min; Gradient: 30%B to 70%B in 10 min; 254 nm to give the title compound (60 mg, 73 %) as a yellow solid.

^{1}H NMR (300 MHz, CD_3OD) δ 1.30-1.45 (m, 3H), 2.82 (s, 3H), 4.17 (s, 2H), 5.13-5.23 (m, 1H), 6.86 – 6.93 (m, 1H), 7.05 (s, 1H), 7.36 (s, 1H), 7.45 (d, *J* = 7.6 Hz, 1H), 7.54 (t, *J* = 7.5 Hz, 1H), 7.66 (s, 1H), 8.00-8.25 (m, 1H); m/z (ESI) 432 $[M+H]^+$.

General procedure for synthesis of compounds 15b-g, 20a-g:

Aldehyde **16** (65 mg, 0.15 mmol) was dissolved in a mixture of methanol and dichloromethane (1:1, 10 mL) and the solution was cooled in ice. Sodium cyanoborohydride (14 mg, 1.5 eq) and acetic acid (43 µL, 5 eq) were added followed by the amine (neat or as a solution; 1 eq) over a period of 15 min. The mixture was allowed to stir overnight at ambient temperature then water (0.5 mL) was added and the mixture was concentrated. The residue was purified by preparative HPLC (Waters XBridge Prep C_{18} OBD or Phenyl OBD column, 5µ silica, 19 mm diameter, 150 mm length), using decreasingly polar mixtures of water (containing 10% NH_4HCO_3) and MeCN as eluents to give the pure products.

(S)-4-Amino-6-((1-(3-methyl-6-(3-((methylamino)methyl)phenyl)-5-oxo-5H-thiazolo[3,2-a]pyridin-7-yl)ethyl)amino)pyrimidine-5-carbonitrile (15b)

^{1}H NMR (300 MHz, CD_3OD) δ 1.27 – 1.43 (m, 3H), 2.76 (s, 3H), 2.81 (d, *J* = 1.1 Hz, 3H), 4.16 – 4.29 (m, 2H), 4.98 – 5.14 (m, 1H), 6.87 (d, *J* = 1.2 Hz, 1H), 7.05 (s, 1H), 7.33 – 7.78 (m, 4H), 7.96 (s, 1H); m/z (ESI) 446 $[M+H]^+$.

(S)-4-Amino-6-((1-(6-(3-((dimethylamino)methyl)phenyl)-3-methyl-5-oxo-5H-thiazolo[3,2-a]pyridin-7-yl)ethyl)amino)pyrimidine-5-carbonitrile (15c)

^{1}H NMR (300 MHz, DMSO) δ 1.24 (d, *J* = 7.0 Hz, 3H), 2.35 (s, 6H), 2.68 (d, *J* = 1.2 Hz, 3H), 3.71 (s, 2H), 4.89 (s, 1H), 6.94 (d, *J* = 1.3 Hz, 1H), 7.00 (s, 1H), 7.1 – 7.34 (m, 4H), 7.36 – 7.44 (m, 1H), 7.52 (d, *J* = 7.2 Hz, 1H), 7.95 (s, 1H), 8.14 (s, 1H); m/z (ESI) 460 $[M+H]^+$.

(S)-4-Amino-6-((1-(6-(3-(((2-methoxyethyl)amino)methyl)phenyl)-3-methyl-5-oxo-5H-thiazolo[3,2-a]pyridin-7-yl)ethyl)amino)pyrimidine-5-carbonitrile (15d)

^{1}H NMR (300 MHz, CD_3OD) δ 1.32 (d, *J* = 6.9 Hz, 3H), 2.79 (d, *J* = 1.1 Hz, 5H), 3.48 (s, 2H), 3.84 (s, 2H), 5.10 (d, *J* = 7.1 Hz, 1H), 6.82 (d, *J* = 1.2 Hz, 1H), 7.01 (s, 1H), 7.22 (m, 1H), 7.34 (d, *J* = 7.5 Hz, 1H), 7.43 (t, *J* = 7.5 Hz, 1H), 7.55 (m, 1H), 7.96-8.01 (m, 1H) (3H obscured); m/z (ESI) 490 $[M+H]^+$.

(S)-4-Amino-6-((1-(6-(3-((isobutyl(methyl)amino)methyl)phenyl)-3-methyl-5-oxo-thiazolo(3,2-a)pyridin-7-yl)ethyl)amino)pyrimidine-5-carbonitrile (15e)

^{1}H NMR (300 MHz, DMSO) δ 0.82 (d, *J* = 6.4 Hz, 6H), 1.22 (d, *J* = 7.0 Hz, 3H), 1.76 (s, 1H), 2.07 (s, 5H), 2.67 (s, 3H), 3.43 (s, 2H), 4.84 – 5.01 (m, 1H), 6.92 (s, 1H), 6.97 (s, 1H), 7.23 (s, 3H), 7.33 (s, 2H), 7.48 (d, *J* = 6.9 Hz, 1H), 7.93 (s, 1H); m/z (ESI) 502 $[M+H]^+$.

(S)-4-Amino-6-((1-(6-(3-(azetidin-1-ylmethyl)phenyl)-3-methyl-5-oxo-5H-thiazolo[3,2-a]pyridin-7-yl)ethyl)amino)pyrimidine-5-carbonitrile (15f)

^{1}H NMR (300 MHz, CD_3OD) δ 1.33 (d, *J* = 7.1 Hz, 3H), 2.22 (s, 2H), 2.68 – 2.9 (m, 3H), 3.54 (s, 4H), 3.85 (s, 2H), 5.06 (s, 1H), 6.83 (d, *J* = 1.1 Hz, 1H), 7.01 (s, 1H), 7.25 (s, 1H), 7.33 (d, *J* = 7.6 Hz, 1H), 7.45 (t, *J* = 7.6 Hz, 1H), 7.56 (s, 1H), 7.96 – 8.02 (m, 1H); m/z (ESI) 472 $[M+H]^+$.

(S)-4-Amino-6-((1-(3-methyl-5-oxo-6-(3-(((4-phenethoxybutyl)amino)methyl)phenyl)-5H-thiazolo[3,2-a]pyridin-7-yl)ethyl)amino)pyrimidine-5-carbonitrile (15g)

^{1}H NMR (400MHz; CD_3OD) δ 1.28-1.42 (3H, m), 1.67-1.79 (4H, d), 2.67-2.86 (5H,m), 2.98-3.09 (2H, m), 3.50-3.51 (2H, m), 3.67.(2H, s), 4.17-4.19 (2H,d), 3.57 (2H,s), 5.00-5.20 (1H, m), 6.89 (1H, s), 7.06 (1H, s), 7.15-7.28 (5H, m),7.44-7.46 (2H, d),7.50-7.75 (2H, m), 8.00 (1H, s); m/z (ESI) 608 $[M+H]^+$.

(S)-4-Amino-6-((1-(6-(3-formylphenyl)-3-methyl-5-oxo-5H-thiazolo[3,2-a]pyridin-7-yl)ethyl)amino)pyrimidine-5-carbonitrile (16)

(3-Formylphenyl)boronic acid (370 mg, 2.47 mmol) was added to (S)-4-amino-6-((1-(6-bromo-3-methyl-5-oxo-5H-thiazolo[3,2-a]pyridin-7-yl)ethyl)amino)pyrimidine-5-carbonitrile (**14**, 500 mg, 1.23 mmol), cesium carbonate (804 mg, 2.47 mmol) and $PdCl_2$(dppf)-CH_2Cl_2 adduct (101 mg, 0.12 mmol) in DME (10 mL) and water (3ml) at 25°C over a period of 15 minutes under nitrogen. The reaction was heated to 100 ºC for 30 minutes in a microwave reactor and cooled to RT. The reaction mixture was quenched with water (10 mL), extracted with EtOAc (3 x 10 mL), the organic layer was dried over Na_2SO_4, filtered and evaporated. The crude product was purified by flash silica chromatography, elution gradient 30 to 50% EtOAc in petroleum ether to give the title compound (400 mg, 75 %) as a white solid.

^{1}H NMR (500 MHz, DMSO-d6) δ 1.26 (d, *J* = 7.1 Hz, 3H), 2.68 (d, *J* = 1.1 Hz, 3H), 4.86 (quint, *J* = 7.0 Hz, 1H), 6.96 (d, *J* = 1.3 Hz, 1H), 7.05 (s, 1H), 7.23 (brs, 2H), 7.56 (d, *J* = 7.1 Hz, 1H), 7.61 – 7.67 (m, 1H), 7.84 – 7.88 (m, 1H), 7.94 (s, 1H), 7.4 – 8.2 (vbrm, 2H), 10.05 (s, 1H). Note: aromatic protons 2 and 6 from the 3-formylphenyl ring are observed as very broad signals in baseline between 7.4-8.2 ppm; ^{13}C NMR (126 MHz, DMSO) δ 18.0, 20.5, 47.7, 67.9, 96.4, 107.8, 115.4, 118.9, 128.0, 128.7, 132.2, 136.0, 137.0, 137.1, 137.6, 152.6, 159.4, 160.7, 161.5, 164.3, 193.2; m/z (ESI) 431 $[M+H]^+$.

(S)-4-Amino-6-((1-(6-(3-(2-(dimethylamino)ethyl)phenyl)-3-methyl-5-oxo-5H-thiazolo[3,2-a]pyridin-7-yl)ethyl)amino)pyrimidine-5-carbonitrile formic acid salt (17)

Step 1

3rd Generation PCy_3 precatalyst[32] (48 mg, 0.07 mmol), (S)-4-amino-6-((1-(6-bromo-3-methyl-5-oxo-5H-thiazolo[3,2-a]pyridin-7-yl)ethyl)amino)pyrimidine-5-carbonitrile (300 mg, 0.74 mmol), tert-butyl 3-(4,4,5,5-tetramethyl-1,3,2-dioxaborolan-2-yl)phenethylcarbamate (514 mg, 1.48 mmol potassium phosphate (471 mg, 2.22 mmol) and $Cy_3P.HBF_4$ (54.5 mg, 0.15 mmol) were mixed in dioxane (12 mL)/water (3 mL) and sealed into a microwave tube. The reaction was heated to 130 °C for 1 hour in the microwave reactor and cooled to RT. The

reaction mixture was diluted with CH_2Cl_2 (150 mL), and washed with water (100 mL×1), and saturated brine (100 mL×1). The organic layer was dried over Na_2SO_4, filtered and evaporated. The residue was purified by flash silica chromatography, elution gradient 20 to 50% EtOAc in petroleum ether to give (S)-tert-butyl 3-(7-(1-((6-amino-5-cyanopyrimidin-4-yl)amino)ethyl)-3-methyl-5-oxo-5H-thiazolo[3,2-a]pyridin-6-yl)phenethylcarbamate (180 mg, 45 %) as a yellow solid.

Step 2

TFA (2.5 mL, 33 mmol) was added to (S)-tert-butyl 3-(7-(1-((6-amino-5-cyanopyrimidin-4-yl)amino)ethyl)-3-methyl-5-oxo-5H-thiazolo[3,2-a]pyridin-6-yl)phenethylcarbamate (180 mg, 0.33 mmol) in CH_2Cl_2 (5 mL) at 25 °C under nitrogen. The resulting mixture was stirred at 25 °C for 4 h. The solvent was removed under reduced pressure and the crude product was purified by preparative HPLC (Phenomenex Gemini-NX axia Prep C18 OBD column, 5µ silica, 19 mm diameter, 100 mm length), using water (containing 1 % TFA) and MeCN as eluents to give (S)-4-amino-6-((1-(6-(3-(2-aminoethyl)phenyl)-3-methyl-5-oxo-5H-thiazolo[3,2-a]pyridin-7-yl)ethyl)amino)pyrimidine-5-carbonitrile (130 mg, 70 %) as a pale yellow solid.

^{1}H NMR (300 MHz, CD_3OD) δ 1.32 – 1.45 (m, 3H), 2.81 (d, J = 0.9 Hz, 3H), 2.9 – 3.1 (m, 2H), 3.15 – 3.3 (m, 2H), 5.03 – 5.21 (m, 1H), 6.88 (s, 1H), 6.99 – 7.58 (m, 5H), 7.96 – 8.13 (m, 1H).

Step 3

Sodium cyanoborohydride (11 mg, 0.18 mmol) was added to (S)-4-amino-6-((1-(6-(3-(2-aminoethyl)phenyl)-3-methyl-5-oxo-5H-thiazolo[3,2-a]pyridin-7-yl)ethyl)amino)pyrimidine-5-carbonitrile (40 mg, 0.09 mmol), formaldehyde (20 mg, 0.27 mmol) and AcOH (0.026 mL, 0.45 mmol) in MeOH (5 mL) at 25 ºC. The resulting mixture was stirred at 25 °C for 3 h. The crude product was purified by preparative HPLC (Phenomenex Gemini-NX axia Prep

C18 OBD column, 5µ silica, 19 mm diameter, 100 mm length), using water (containing 1% Formic acid) and MeCN as eluents to give the title compound (9 mg, 20 %) as a pale yellow solid.

^{1}H NMR (300 MHz, CD_3OD) δ 1.26 – 1.41 (m, 3H), 2.74 – 2.89 (m, 9H), 2.96 – 3.11 (m, 2H), 3.19 – 3.36 (m, 2H), 4.98 – 5.16 (m, 1H), 6.84 – 6.86 (m, 1H), 7.00 – 7.07 (m, 1H), 7.14 – 7.24 (m, 1H), 7.25 – 7.34 (m, 1H), 7.38 – 7.57 (m, 2H), 7.95 (s, 1H), 8.54 (s, 1H); m/z (ESI) 490 $[M+H]^+$.

(S)-4-Amino-6-((1-(6-(3-(2-(dimethylamino)ethoxy)phenyl)-3-methyl-5-oxo-5H-thiazolo[3,2-a]pyridin-7-yl)ethyl)amino)pyrimidine-5-carbonitrile formic acid salt (18)

Step 1

3rd Generation PCy_3 precatalyst[32] (48.1 mg, 0.07 mmol), $PCy_3.HBF_4$ (54.5 mg, 0.15 mmol), (S)-4-amino-6-((1-(6-bromo-3-methyl-5-oxo-5H-thiazolo[3,2-a]pyridin-7-yl)ethyl)amino)pyrimidine-5-carbonitrile (14, 100 mg, 0.25 mmol), 3-(4,4,5,5-tetramethyl-1,3,2-dioxaborolan-2-yl)phenol (163 mg, 0.74 mmol) and K_3PO_4 (157 mg, 0.74 mmol) were dissolved in dioxane (12 mL)/H_2O (2mL) and sealed into a microwave tube. The reaction was heated to 130 ºC for 1 h. The reaction mixture was diluted with CH_2Cl_2 (200 mL), and washed sequentially with saturated $NaHCO_3$ (100 mL), water (100 mL), and saturated brine (100 mL). The organic layer was dried over Na_2SO_4, filtered and evaporated. The crude product was purified by preparative HPLC (Phenomenex Gemini-NX axia Prep C_{18} OBD column, 5µ, 19 × 100 mm; gradient MeCN in 1% aq TFA) to give (S)-4-Amino-6-((1-(6-(3-hydroxyphenyl)-3-methyl-5-oxo-5H-thiazolo[3,2-a]pyridin-7-yl)ethyl)amino)pyrimidine-5-carbonitrile (80 mg, 61 %) as a yellow solid.

^{1}H NMR (400 MHz,CD_3OD) δ 1.40 (d, *J* = 6.8 Hz, 3H), 2.79 (s, 3H), 5.22 (s, 1H), 6.76 (s, 2H), 6.84 (s, 1H), 6.99 (s, 2H), 7.24 (t, *J* = 7.8, 7.8 Hz, 1H), 8.07 (s, 1H).

Step 2

DEAD (75 mg, 0.43 mmol) was added to (S)-4-amino-6-((1-(6-(3-hydroxyphenyl)-3-methyl-5-oxo-5H-thiazolo[3,2-a]pyridin-7-yl)ethyl)amino)pyrimidine-5-carbonitrile (60 mg, 0.14 mmol), 2-(dimethylamino)ethanol (19 mg, 0.22 mmol) and triphenylphosphine (113 mg, 0.43 mmol) in THF (10 mL) at 0 ºC over a period of 2 minutes under nitrogen. The resulting solution was stirred at 40 °C for 12 hours. The solvent was removed under reduced pressure and the crude product was purified by preparative HPLC (XBridge Prep C_{18} OBD column, 5µ silica, 19 mm diameter, 150 mm length), using water (containing 0.05 % Formic acid) and MeCN as eluents to give the title compound (10 mg, 13 %) as a white solid.

^{1}H NMR (300 MHz, CD_3OD) δ 1.34 (d, J = 7.1 Hz, 3H), 2.58 (s, 6H), 2.80 (s, 3H), 3.03 – 3.14 (m, 2H), 4.15 – 4.29 (m, 2H), 5.07 – 5.19 (m, 1H), 6.8 – 6.92 (m, 2H), 6.93 – 6.99 (m, 1H), 7.00 (s, 1H), 7.15 – 7.25 (m, 1H), 7.36 (t, J = 7.9 Hz, 1H), 7.95 (s, 1H), 8.52 (s, 1H); m/z (ESI) 474 $[M+H]^+$.

(S)-4-Amino-6-((1-(3-methyl-5-oxo-6-(3-((1-(3,3,3-trifluoropropyl)piperidin-4-yl)methyl)phenyl)-5H-thiazolo[3,2-a]pyridin-7-yl)ethyl)amino)pyrimidine-5-carbonitrile (19)

Step 1

$PdCl_2$(dppf)-CH_2Cl_2 adduct (100 mg, 0.12 mmol), (S)-4-amino-6-((1-(6-bromo-3-methyl-5-oxo-5H-thiazolo[3,2-a]pyridin-7-yl)ethyl)amino)pyrimidine-5-carbonitrile (14, 250 mg, 0.62 mmol), tert-butyl 4-(3-(4,4,5,5-tetramethyl-1,3,2-dioxaborolan-2-yl)benzyl)piperidine-1-carboxylate[33] (990 mg, 2.47 mmol) and cesium carbonate (804 mg, 2.47 mmol) were dissolved in dioxane (12 mL)/water (4 mL) and sealed into a microwave tube. The reaction was heated to 130 ºC for 2 hours in a microwave reactor and cooled to RT. The reaction mixture was diluted with EtOAc (100 mL), and washed sequentially with water (100 mL × 1) and saturated brine (100 mL × 1). The organic layer was dried over Na_2SO_4, filtered and evaporated. The residue was purified by preparative TLC (EtOAc: petroleum ether = 1: 1), to

give tert-butyl 4-[3-(7-{(1S)-1-[(6-amino-5-cyanopyrimidin-4-yl)amino]ethyl}-3-methyl-5-oxo-5H-[1,3]thiazolo[3,2-a]pyridin-6-yl)benzyl]piperidine-1-carboxylate (260 mg, 70 %) as a yellow solid.

Step 2

TFA (1.5 mL, 19 mmol) was added to (S)-tert-butyl 4-(3-(7-(1-((6-amino-5-cyanopyrimidin-4-yl)amino)ethyl)-3-methyl-5-oxo-5H-thiazolo[3,2-a]pyridin-6-yl)benzyl)piperidine-1-carboxylate (260 mg, 0.43 mmol) in CH_2Cl_2 (20 mL) at 0 °C over a period of 15 minutes under nitrogen. The resulting solution was stirred for 12 hours. The reaction mixture was quenched with saturated $NaHCO_3$ (20 mL), extracted with CH_2Cl_2 (3 × 10 mL), the organic layer was dried over Na_2SO_4, filtered and evaporated to give (S)-4-amino-6-((1-(3-methyl-5-oxo-6-(3-(piperidin-4-ylmethyl)phenyl)-5H-thiazolo[3,2-a]pyridin-7-yl)ethyl)amino)pyrimidine-5-carbonitrile (230 mg, 106 %) as a yellow solid that was used without further purification.

Step 3

$NaCNBH_3$ (15 mg, 0.24 mmol) was added to (S)-4-amino-6-((1-(3-methyl-5-oxo-6-(3-(piperidin-4-ylmethyl)phenyl)-5H-thiazolo[3,2-a]pyridin-7-yl)ethyl)amino)pyrimidine-5-carbonitrile (60 mg, 0.12 mmol), 3,3,3-trifluoropropanal (53.8 mg, 0.48 mmol) and AcOH (0.034 mL, 0.60 mmol) in a mixture of CH_2Cl_2 (5 mL) and MeOH (5 mL) were added at 25 °C over a period of 15 minutes. The resulting mixture was stirred at 45 °C for 12 hours. The solvent was evaporated and the residue was purified by preparative HPLC (XBridge Prep C_{18} OBD column, 5µ silica, 19 mm diameter, 150 mm length), using decreasingly polar mixtures of water (containing 0.5% TFA) and MeCN as eluents to give the title compound (20 mg, 16 %) as a yellow solid.

^{1}H NMR (300 MHz, CD_3OD) δ 1.27 – 1.41 (m, 10H), 1.42 – 1.61 (m, 2H), 1.88 – 2.08 (m, 4H), 2.66 (d, J = 6.6 Hz, 2H), 2.80 (d, J = 1.0 Hz, 3H), 2.87 – 3.06 (m, 3H), 3.36 – 3.52 (m,

3H), 5.06 – 5.21 (m, 1H), 6.86 (d, *J* = 1.2 Hz, 1H), 7.02 (s, 1H), 7.07 – 7.22 (m, 2H), 7.33 – 7.44 (m, 2H), 8.04 (s, 1H); m/z (ESI) 596 $[M+H]^+$.

Compounds 20a – 20g synthesised following procedure described earlier for 15b-g

((S)-4-Amino-6-((1-(3-methyl-6-(3-(((2-morpholinoethyl)amino)methyl)phenyl)-5-oxo-5H-thiazolo[3,2-a]pyridin-7-yl)ethyl)amino)pyrimidine-5-carbonitrile (20a)

^{1}H NMR (300 MHz, DMSO-d6) δ 1.22 (d, *J* = 7.0 Hz, 3H), 1.94 – 2.4 (m, 7H), 2.53 – 2.62 (m, 2H), 2.68 (s, 3H), 3.4 – 3.56 (m, 4H), 3.72 (s, 2H), 4.85 – 4.99 (m, 1H), 6.92 (d, *J* = 1.2 Hz, 1H), 6.97 (s, 1H), 7.02 – 7.61 (m, 7H), 7.97 (s, 1H); m/z (ESI) 545 $[M+H]^+$.

(S)-4-Amino-6-((1-(6-(3-((4-(dimethylamino)piperidin-1-yl)methyl)phenyl)-3-methyl-5-oxo-5H-thiazolo[3,2-a]pyridin-7-yl)ethyl)amino)pyrimidine-5-carbonitrile (20b)

^{1}H NMR (500 MHz, DMSO-d6) δ 1.22 (d, *J* = 7.0 Hz, 3H), 1.27 – 1.40 (m, 2H), 1.57 – 1.75 (m, 2H), 1.83 – 1.98 (m, 2H), 2.00 – 2.12 (m, 1H), 2.15 (s, 6H), 2.68 (s, 3H), 2.76 – 2.91 (m, 2H), 3.44 (s, 2H), 4.84 – 4.96 (m, 1H), 6.91 – 6.94 (m, 1H), 6.98 (s, 1H), 7.00 – 7.47 (m, 6H), 7.48 (d, *J* = 7.1 Hz, 1H), 7.94 (s, 1H); ^{13}C NMR (126 MHz, DMSO-d6) δ 18.14, 20.51, 27.90 (2C), 41.33 (2C), 47.72, 52.36, 52.46, 61.68, 62.18, 67.90, 96.23, 107.55, 115.44, 120.39, 127.19, 127.57, 129.19, 130.99, 135.74, 137.53, 138.11, 148.11, 152.42, 159.40, 160.87, 161.56, 164.36; m/z (ESI) 543 $[M+H]^+$; HRMS calculated for $C_{29}H_{35}N_8OS$ [(M + H)+], 543.2649; found, 543.2641

(S)-4-Amino-6-((1-(6-(3-((4-((isobutyl(methyl)amino)methyl)piperidin-1-yl)methyl)phenyl)-3-methyl-5-oxo-5H-thiazolo[3,2-a]pyridin-7-yl)ethyl)amino)pyrimidine-5-carbonitrile (20c)

^{1}H NMR (400 MHz, CD_3OD) δ 0.88 (d, *J* = 6.0 Hz, 6H), 1.18-1.35 (m, 5H), 1.50-1.82 (m, 4H), 2.0-2.35 (m, 9H), 2.71 – 2.87 (m, 3H), 3.06 (s, 2H), 3.71 (s, 2H), 5.05 (s, 1H), 6.83 (s, 1H), 7.01 (s, 1H), 7.26 (s, 1H), 7.35 (d, *J* = 7.7 Hz, 1H), 7.44 (t, *J* = 7.6, 7.6 Hz, 1H), 7.52-7.61 (m, 1H), 7.92-8.02 (m, 1H) 3H obscured; m/z (ESI) 599 $[M+H]^+$.

(S)-4-Amino-6-((1-(3-methyl-6-(3-((4-(methyl(3,3,3-trifluoropropyl)amino)piperidin-1-yl)methyl)phenyl)-5-oxo-5H-thiazolo[3,2-a]pyridin-7-yl)ethyl)amino)pyrimidine-5-carbonitrile (20d)

^{1}H NMR (400 MHz, CD_3OD) δ 1.34-1.46 (m, 3H), 2.14 (s, 2H), 2.28-2.41 (m, 2H), 2.79-2.94 (m, 8H), 3.18 (t, *J* = 12.2 Hz, 2H), 3.47-3.53 (m, 2H), 3.63-3.86 (m, 3H), 4.41 (d, *J* = 15.0 Hz, 2H), 5.00-5.21 (1H, m), 6.90 (s, 1H), 7.05 (s, 1H), 7.39-7.76 (m, 4H), 8.10 (s, 1H); 3H obscured; ^{19}F NMR (376 MHz; CD_3OD) δ -66.6; m/z (ESI) 625 $[M+H]^+$.

(S)-4-Amino-6-((1-(3-methyl-6-(3-((4-(2-morpholinoethyl)piperazin-1-yl)methyl)phenyl)-5-oxo-5H-thiazolo[3,2-a]pyridin-7-yl)ethyl)amino)pyrimidine-5-carbonitrile (20e)

^{1}H NMR (300 MHz, CD_3OD) δ 1.24 – 1.57 (m, 3H), 2.35 – 2.63 (m, 2H), 2.71 – 2.95 (m, 5H), 3.03 – 3.31 (m, 7H), 3.44 – 3.72 (m, 5H), 3.83 – 4.08 (m, 4H), 4.3 – 4.52 (m, 2H), 5.16 (s, 1H), 6.91 (s, 1H), 7.07 (s, 1H), 7.36 – 7.55 (m, 2H), 7.54 – 7.67 (m, 1H), 7.78 (s, 1H), 8.06 (s, 1H); m/z (ESI) 614 $[M+H]^+$.

(S)-4-amino-6-((1-(6-(3-((4-(isobutyl(methyl)amino)piperidin-1-yl)methyl)phenyl)-3-methyl-5-oxo-5H-thiazolo[3,2-a]pyridin-7-yl)ethyl)amino)pyrimidine-5-carbonitrile (20f)

^{1}H NMR (500 MHz, DMSO-d6) δ 0.80 (d, *J* = 6.6 Hz, 6H), 1.22 (d, *J* = 7.0 Hz, 3H), 1.29 – 1.44 (m, 2H), 1.46 – 1.66 (m, 3H), 1.81 – 1.95 (m, 2H), 2.05 (d, *J* = 6.9 Hz, 2H), 2.10 (s, 3H), 2.16 – 2.28 (m, 1H), 2.68 (s, 3H), 2.76 – 2.91 (m, 2H), 3.44 (brs, 2H), 4.84 – 5.01 (brm, 1H), 6.91 – 6.94 (m, 1H), 6.98 (s, 1H), 7.01 – 7.45 (m, 6H), 7.47 (d, *J* = 7.0 Hz, 1H), 7.94 (s, 1H); ^{13}C NMR (126 MHz, DMSO-d6) δ 18.14, 20.49, 20.66 (2C), 26.03, 27.41 (2C), 38.04, 47.71, 52.93 (2C), 61.08, 61.40, 62.23, 67.90, 96.22, 107.55, 115.44, 120.38, 127.14, 127.54, 129.20, 130.92, 135.72, 137.53, 138.24, 148.11, 152.43, 159.39, 160.88, 161.56, 164.35; m/z (ESI) 585 $[M+H]^+$; HRMS calculated for $C_{32}H_{41}N_8OS$ [(M + H)+], 585.3124; found, 585.3109

(S)-4-Amino-6-((1-(3-methyl-6-(3-((4-((methyl(pyridin-2-ylmethyl)amino)methyl)piperidin-1-yl)methyl)phenyl)-5-oxo-5H-thiazolo[3,2-a]pyridin-7-yl)ethyl)amino)pyrimidine-5-carbonitrile formic acid salt (20g)

^{1}H NMR (400 MHz, CD_3OD) δ 1.18 – 1.48 (m, 5H), 1.82 – 2.17 (m, 3H), 2.33 (s, 3H), 2.41 (d, *J* = 5.5 Hz, 2H), 2.81 (s, 3H), 2.9 – 3.05 (m, 2H), 3.39 – 3.61 (m, 2H), 3.74 (s, 2H), 4.17 – 4.37 (m, 2H), 4.93 – 5.16 (m, 1H), 6.87 (s, 1H), 7.05 (s, 1H), 7.3 – 7.35 (m, 1H), 7.35 – 7.79 (m, 5H), 7.79 – 7.86 (m, 1H), 7.96 (s, 1H), 8.42 (brs, 1H), 8.48 (d, *J* = 4.4 Hz, 1H); m/z (ESI) 634 $[M+H]^+$.

(S)-4-Amino-6-((1-(6-(3-((ethyl(2-morpholinoethyl)amino)methyl)phenyl)-3-methyl-5-oxo-5H-thiazolo[3,2-a]pyridin-7-yl)ethyl)amino)pyrimidine-5-carbonitrile (20h)

Sodium cyanoborohydride (23 mg, 0.37 mmol) was added to (S)-4-amino-6-((1-(3-methyl-6-(3-(((2-morpholinoethyl)amino)methyl)phenyl)-5-oxo-5H-thiazolo[3,2-a]pyridin-7-yl)ethyl)amino)pyrimidine-5-carbonitrile (20a, 100 mg, 0.18 mmol), acetaldehyde (12 mg, 0.28 mmol) and acetic acid (0.053 mL, 0.92 mmol) in CH_2Cl_2 (5 mL) and MeOH (10 mL) at 25 °C. The resulting mixture was stirred at 25 °C for 12 hours. The solvent was removed under reduced pressure. The crude product was purified by preparative HPLC (Phenomenex Gemini-NX axia Prep C18 OBD column, 5µ silica, 19 mm diameter, 100 mm length), using decreasingly polar mixtures of water (containing 1% NH_4HCO_3) and MeCN as eluents to give the title compound (55 mg, 52 %) as a white solid.

^{1}H NMR (300 MHz, CD_3OD): δ 1.05 - 1.13 (m, 3H), 1.23 - 1.33 (m, 3H), 2.38 - 2.80 (m, 10H), 2.85 (s, 3H), 3.54 - 3.84 (m, 6H), 5.03 - 5.12 (m, 1H), 6.81 (d, *J* = 1.2 Hz, 1H), 6.99 (s, 1H), 7.14 - 7.67 (m, 4H), 7.94 - 8.02 (m, 1H); m/z (ESI) 573 $[M+H]^+$.

(S)-4-Amino-6-((1-(6-(3-(((3-((4-chlorobenzyl)(methyl)amino)propyl)(methyl)amino)methyl)phenyl)-3-methyl-5-oxo-5H-thiazolo[3,2-a]pyridin-7-yl)ethyl)amino)pyrimidine-5-carbonitrile (20i)

Prepared from aldehyde **16** and N^1-(4-chlorobenzyl)-N^1-methylpropane-1,3-diamine according to the standard procedure followed by a reductive amination with formaldehyde following the procedure of Example **20d** step 2.

^{1}H NMR (400MHz; CD_3OD): δ 1.28 (s, 3H), 1.72 (s, 2H), 2.12 (d, *J* = 18.0 Hz, 3H), 2.30-2.40 (m, 2H), 2.63-2.74 (m, 2H), 2.78 (s, 3H), 3.43 (d, *J* = 20.4 Hz, 2H), 3.84 (s, 2H), 5.08 (s, 1H), 6.81 (s, 1H), 6.99 (s, 1H), 7.23 (s, 5H), 7.34 (d, *J* = 7.6 Hz, 1H), 7.44 (t, *J* = 7.6 Hz, 1H), 7.59 (s, 1H), 7.99 (s, 1H); m/z (ESI) 627/629 (Cl pattern) $[M+H]^+$.

4-Amino-6-(((S)-1-(6-(3-(((3-((2R,6S)-2,6-dimethylmorpholino)propyl)(methyl)amino)methyl)phenyl)-3-methyl-5-oxo-5H-thiazolo[3,2-a]pyridin-7-yl)ethyl)amino)pyrimidine-5-carbonitrile (20j)

Prepared from aldehyde **16** and 3-((2R,6S)-2,6-dimethylmorpholino)propan-1-amine according to the standard procedure followed by a reductive amination with formaldehyde following the procedure of Example **20d** step 2.

^{1}H NMR (300MHz; CD_3OD) δ 1.24 (d, *J* = 6.3 Hz, 6H), 1.31 – 1.53 (m, 3H), 2.15 – 2.37 (m, 2H), 2.69 (t, *J* = 11.5, 11.5 Hz, 2H), 2.78 – 2.86 (m, 3H), 2.93 (s, 3H), 3.1 – 3.24 (m, 2H), 3.24 – 3.31 (m, 2H), 3.41 – 3.56 (m, 2H), 3.8 – 3.98 (m, 2H), 4.34 – 4.54 (m, 2H), 4.99 – 5.25 (m, 1H), 6.90 (s, 1H), 7.06 (s, 1H), 7.34 – 7.82 (m, 4H), 8.12 (s, 1H); m/z (ESI) 601 $[M+H]^+$.

(S)-4-amino-6-((1-(6-(3-(((4-(benzyl(methyl)amino)butyl)(methyl)amino)methyl)phenyl)-3-methyl-5-oxo-5H-thiazolo[3,2-a]pyridin-7-yl)ethyl)amino)pyrimidine-5-carbonitrile (20k)

Step 1

Sodium cyanoborohydride (88 mg, 1.39 mmol) was added in one portion to (S)-4-amino-6-((1-(6-(3-formylphenyl)-3-methyl-5-oxo-5H-thiazolo[3,2-a]pyridin-7-yl)ethyl)amino)pyrimidine-5-carbonitrile (300 mg, 0.70 mmol), 4,4-diethoxybutan-1-amine (337 mg, 2.09 mmol) and AcOH (0.2 mL, 3.48 mmol) in CH_2Cl_2 (10 mL) and MeOH (10ml)

at 25 °C over a period of 15 minutes under nitrogen. The resulting mixture was stirred at 25 ºC for 2 hours. The solvent was removed under reduced pressure and the residue was quenched with saturated $NaHCO_3$ (10 mL), extracted with CH_2Cl_2 (3 x 10 mL), the organic layer was dried over Na_2SO_4, filtered and evaporated to give (S)-4-amino-6-((1-(6-(3-(((4,4-diethoxybutyl)amino)methyl)phenyl)-3-methyl-5-oxo-5H-thiazolo[3,2-a]pyridin-7-yl)ethyl)amino)pyrimidine-5-carbonitrile (380 mg, 95 %) as a yellow liquid.

The product was used in the next step directly without further purification.

Step 2

Sodium cyanoborohydride (87 mg, 1.39 mmol) was added in one portion to (S)-4-amino-6-((1-(6-(3-(((4,4-diethoxybutyl)amino)methyl)phenyl)-3-methyl-5-oxo-5H-thiazolo[3,2-a]pyridin-7-yl)ethyl)amino)pyrimidine-5-carbonitrile (400 mg, 0.69 mmol), formaldehyde (31 mg, 1.0 mmol) and acetic acid (209 mg, 3.47 mmol) in MeOH (20 mL) at 25 °C over a period of 25 minutes under nitrogen. The resulting mixture was stirred at 25 °C for 2 hours. The reaction mixture was quenched with saturated $NaHCO_3$ (25 mL) and extracted with EtOAc (3 x 25 mL). The organic layer was dried over Na_2SO_4, filtered and evaporated to give (S)-4-amino-6-((1-(6-(3-(((4,4-diethoxybutyl)(methyl)amino)methyl)phenyl)-3-methyl-5-oxo-5H-thiazolo[3,2-a]pyridin-7-yl)ethyl)amino)pyrimidine-5-carbonitrile (320 mg, 78 %) as a yellow oil.

The product was used in the next step directly without further purification.

Step 3

TFA (3.38 mL, 44 mmol) was added portionwise to a cold (0 ºC) solution of (S)-4-amino-6-((1-(6-(3-(((4,4-diethoxybutyl)(methyl)amino)methyl)phenyl)-3-methyl-5-oxo-5H-thiazolo[3,2-a]pyridin-7-yl)ethyl)amino)pyrimidine-5-carbonitrile (400 mg, 0.68 mmol) in $CHCl_3$ (40 mL) and H_2O (5ml) over a period of 15 minutes. The resulting solution was stirred at 25 ºC for 2 hours. The reaction mixture was quenched with saturated $NaHCO_3$ (25 mL),

extracted with CH_2Cl_2 (3 × 25 mL), the organic layer was dried over Na_2SO_4, filtered and evaporated to give (S)-4-amino-6-((1-(3-methyl-6-(3-((methyl(4-oxobutyl)amino)methyl)phenyl)-5-oxo-5H-thiazolo[3,2-a]pyridin-7-yl)ethyl)amino)pyrimidine-5-carbonitrile (350 mg, 100 %) as a yellow solid.

Step 4-(S)-4-amino-6-((1-(6-(3-(((4-(benzyl(methyl)amino)butyl)(methyl)amino)methyl)phenyl)-3-methyl-5-oxo-5H-thiazolo[3,2-a]pyridin-7-yl)ethyl)amino)pyrimidine-5-carbonitrile

Sodium cyanoborohydride (24 mg, 0.39 mmol) was added in one portion to (S)-4-amino-6-((1-(3-methyl-6-(3-((methyl(4-oxobutyl)amino)methyl)phenyl)-5-oxo-5H-thiazolo[3,2-a]pyridin-7-yl)ethyl)amino)pyrimidine-5-carbonitrile (100 mg, 0.19 mmol), N-methyl-1-phenylmethanamine (47 mg, 0.39 mmol) and acetic acid (58 mg, 0.97 mmol) in CH_2Cl_2 (10 mL) and MeOH (10ml) at 25 °C over a period of 15 minutes under nitrogen. The resulting solution was stirred at 25 ºC for 12 hours. The solvent was removed under reduced pressure. The crude product was purified by preparative HPLC (XBridge Prep C18 OBD column, 5µ silica, 19 mm diameter, 150 mm length; water (0.5% TFA) and MeCN) to give the title compound (89 mg, 62 %) as a yellow solid.

^{1}H NMR (300MHz; CD_3OD) δ 1.36-1.42 (3H, m), 1.76 - 1.90 (4H, m), 2.73-2.80 (6H, m), 2.90 (3H, brs), 3.08-3.31 (4H, m), 4.30-4.49 (4H, m), 4.98-5.18 (1H, m), 6.89 (1H, s), 7.07 (1H, s), 7.45-7.77 (9H, m), 8.05 (1H, s) 4H obscured; m/z (ESI) 621 $[M+H]^+$.

4-Amino-6-(((S)-1-(6-(3-(((4-((2S,6R)-2,6-dimethylmorpholino)butyl)(methyl)amino)methyl)phenyl)-3-methyl-5-oxo-5H-thiazolo[3,2-a]pyridin-7-yl)ethyl)amino)pyrimidine-5-carbonitrile (20l)

Prepared from (S)-4-amino-6-((1-(3-methyl-6-(3-((methyl(4-oxobutyl)amino)methyl)phenyl)-5-oxo-5H-thiazolo[3,2-a]pyridin-7-

yl)ethyl)amino)pyrimidine-5-carbonitrile (step 3 **20k**) and (2S,6R)-2,6-dimethylmorpholine under the conditions of step 4 **20k.**

^{1}H NMR (300MHz; CD_3OD) δ 1.24 (d, J = 6.3 Hz, 5H), 1.29 – 1.49 (m, 3H), 1.7 – 1.96 (m, 4H), 2.67 (t, J = 11.5 Hz, 2H), 2.82 (s, 3H), 2.89 (s, 3H), 3.1 – 3.31 (m, 5H), 3.4 – 3.52 (m, 2H), 3.79 – 3.96 (m, 2H), 4.25 – 4.56 (m, 2H), 4.98 – 5.25 (m, 1H), 6.91 (s, 1H), 7.07 (s, 1H), 7.38 – 7.82 (m, 4H), 8.09 (s, 1H); m/z (ESI) 615 $[M+H]^+$.

Enzymatic activity assay for recombinant human PI3Kα, β, δ and γ.

The activity of recombinant human PI3Kγ ((aa144-1102)-6His) and PI3Kα, β, δ (6-His(p110– p85α) was determined by measuring the ADP level after phosphorylation of DiC_8-PIP_2 using a commercially available ADP-Glo ™ kit from Promega. The assay was carried out in white low volume 384 well plates in a final volume of 14 µl at R.T. The assay conditions contained the following: 50 mM Tris buffer pH 7.4, 2.1 mM DTT, 3 mM $MgCl_2$, 0.05 % CHAPS, 20 µM ATP, 80 µM DiC_8-PIP_2 and 1.2 nM PI3Kα, β, γ or 0.6 nM PI3Kδ. Potential inhibitors were made up in DMSO and then diluted in the assay to give a final concentration of not exceeding 1% (v/v) DMSO. A 10-point half-log dilution series of the inhibitors (highest concentration typically 0.1 µM for δ,γ and 33 µM for α, β) was tested and the pIC_{50} determined using a 4-paramater logistic equation in a non-linear curve fitting routine. Routinely, inhibitors were pre-incubated with 3 µl of enzyme for 15 min prior to the addition of 2 µl substrate mixture for a further 60 min enzyme reaction. The phosphorylation was stopped with the addition of 3 µl ADP-Glo™ reagent (stop solution) followed by a 40 min incubation. Prior to detection 6 µl of ADP-Glo™ Kinase Detection Reagent was added and the plates were read in a micro plate reader using a Luminescence filter. All additions were followed by a short centrifugation step.

Inhibition of cellular activity in JeKo-1 cells.

PI3Kδ inhibitors were identified by measuring the phosphorylation of AKT (at Ser473) using TR-FRET technology (Phospho-AKT (Ser473) kit, Cisbio) in JeKo-1 cells - Lymphoblast B cell line (ATCC). Cryogenically preserved cells were thawed rapidly in RPMI 1640 medium (10 % FBS, 2 mM Glutamine) at 37 °C. Cells were plated in white low volume 384 well plates at a density of 1.25E6 cells/ml in assay buffer (RPMI 1640 medium, 2 mM Glutamine). Potential inhibitors were made up in DMSO and then diluted in the assay to give a final concentration of not exceeding 1% (v/v) DMSO. A 10-point half-log dilution series of the inhibitors (highest concentration typically 1 µM) was tested and the pIC_{50} determined using a 4-paramater logistic equation in a non-linear curve fitting routine. Inhibitors were incubated with 8 µl of cells for 60 min at 30 °C previously stimulated with 2 µl Anti-IgM (250 ng/ml) in assay buffer. After an incubation of 10 min at 37 °C the cells were lysed for 30 min at RT on a plate shaker at 500 rpm. A 5 µl mix of d2/cryptate was added to the plates and the FRET signals were read in a micro plate reader after 3-4 h at 620 nm & 665 nm.

Rat intratracheal instillation to determine the lung retention of inhaled compounds

All rat experiments were approved by the Gothenburg Ethics Committee for Experimental Animals in Sweden and conform to Directive 2010/63/EU, ethical license No. 135-2014

The lung half-lives and percentage remaining in the lung at 4 h of the compounds were determined after intratracheal instillation as previously described.[34] The terminal phase of the time-concentration curve was used for determination of the half-lives. Briefly, a special cannula, connected to a syringe, was inserted in the trachea at the first bifurcation and 0.5 mL/kg was instilled into the trachea. Sampling of lungs were made at predefined time-points, and the lungs were placed on ice and stored at - 20 °C until homogenization (Bertin technologies) prior to analysis with LC-MS/MS.

Target engagement *in vivo* model

All mouse experiments were approved by the Gothenburg Ethics Committee for Experimental Animals in Sweden and conform to Directive 2010/63/EU, ethical license No. 47-2013

The T-cell receptor transgenic mouse (OT-II; C57BL/6-Tg(TcraTcrb)425Cbn/Crl[28] was ordered (Charles River, Sulzfeld, Germany) as 8-10 weeks of age, randomized upon arrival, and allowed to acclimatise at least 1 week in the animal facility before the experimental start.

The mice were OVA (Albumin chicken egg, grade V (Sigma-Aldrich), Sweden, #A5503) challenged on day 0 by intranasal administration (50 µg/mouse in 50µL saline) to stimulate and recruit inflammatory cells locally to the lung. Five days later, the lung T-cells were activated by the intranasal administration of 0.5 µg anti-CD3 (clone 145-2C11, Cat# 553057 from BD Bioscience) per mouse in 50µL saline. Isotype Hamster IgG1 (clone A19-3 Cat# 553968 from BD Bioscience) was used as control. The animals were (2.5 mL/kg Bw) treated intratracheally with PI3Kδ inhibitor (or vehicle for control animals) 18 hours prior to anti-CD3 challenge. The bronchoalveolar lung lavage (BAL) cells were isolated 6 hours after anti-CD3 challenge, fixed by Phosflow Fix buffer I and permeabilised by permeabilisation buffer III (both from BD Bioscience). Cells were then stained with phospho-S6 Ribosomal Protein (Ser235/236) (D57.2.2E) XP®Rabbit mAb (AlexaFluor488 Conjugate, Cell Signaling Technology) and data were collected using a LSRFortessa cell analyser (BD Biosciences). Data analysis was performed using FlowJo (Tree Star) software.

Supporting Information

Ligand diagrams for the crystal structures; Kinase selectivity profile for **20b** & **20f**; Analytical HPLC conditions; HPLCMS results; Synthesis procedures for compounds **1** & **2**; NMR spectra for compounds **3**–**20l**; HPLCMS traces for compounds **20b** & **20f**

This material is available free of charge via the Internet at http://pubs.acs.org

AUTHOR INFORMATION

Corresponding Author

*(MWDP) e-mail matthew.perry@astrazeneca.com

Present Addresses

Neil Holden : University of Lincoln, Brayford Pool, Lincoln, Lincolnshire, LN6 7TS, United Kingdom

Author Contributions

The manuscript was written through contributions of all authors. All authors have given approval to the final version of the manuscript.

ACKNOWLEDGMENT

We would like to thank our colleagues in the analytical and purification departments at both AstraZeneca R&D Mölndal and Pharmaron Beijing for their support with purification and characterisation of the compounds described in this work. We would also like to thank the colleagues at AstraZeneca and Pharmaron whose testing of the compounds provided the results which are described.

ABBREVIATIONS

DIEA diisopropylethylamine; ESI electrospray ionization; EtOAc ethyl acetate; PE petroleum ether ; TEA triethylamine.

COMPOUND CODE NUMBERS

Crystal structures for compounds **13** (5NCY) and **15c** (5NCZ) have been deposited with the PDB. Authors will release the atomic coordinates and experimental data upon article publication.

REFERENCES

(1) Fruman, D.; Rommel, C. PI3K and Cancer: Lessons, Challenges and Opportunities. *Nat. Rev. Drug Discovery* **2014**, *13*, 140–156.

(2) Yap, T.; Bjerke, L.; Clarke, P.; Workman, P. Drugging PI3K in Cancer: Refining Targets and Therapeutic Strategies. *Curr. Opin. Pharmacol.* **2015**, *23*, 98–107.

(3) Cushing, T. D.; Metz, D. P.; Whittington, D.; McGee, L. R. PI3Kδ and PI3Kγ as Targets for Autoimmune and Inflammatory Diseases. *J. Med. Chem.* **2012**, *55*, 8559–8581.

(4) Rowan, W. C.; Smith, J. L.; Affleck, K.; Amour, A. Targeting Phosphoinositide 3-Kinase δ for Allergic Asthma. *Biochem. Soc. Trans.* **2012**, *40*, 240–245.

(5) Puri, K. D.; Gold, M. R. Selective Inhibitors of Phosphoinositide 3-Kinase Delta: Modulators of B-Cell Function with Potential for Treating Autoimmune Inflammatory Diseases and B-Cell Malignancies. *Front. Immunol.* **2012**, *3*, 256.

(6) Sriskantharajah, S.; Hamblin, N.; Worsley, S.; Calver, A. R.; Hessel, E. M.; Amour, A. Targeting Phosphoinositide 3-Kinase δ for the Treatment of Respiratory Diseases. *Ann. N. Y. Acad. Sci.* **2013**, *1280*, 35–39.

(7) Hawkins, P. T.; Stephens, L. R. PI3K Signalling in Inflammation. *Biochim. Biophys. Acta - Mol. Cell Biol. Lipids* **2015**, *1851*, 882–897.

(8) So, L.; Fruman, D. PI3K Signalling in B- and T-Lymphocytes: New Developments and Therapeutic Advances. *Biochem. J.* **2012**, *442*, 465–481.

(9) Fung-Leung, W.-P. Phosphoinositide 3-Kinase Gamma in T Cell Biology and Disease Therapy. *Ann. N. Y. Acad. Sci.* **2013**, *1280*, 40–43.

(10) Vanhaesebroeck, B.; Whitehead, M. A.; Piñeiro, R. Molecules in Medicine Mini-Review: Isoforms of PI3K in Biology and Disease. *J. Mol. Med.* **2016**, *94*, 5–11.

(11) Markham, A. Idelalisib: First Global Approval. *Drugs* **2014**, *74*, 1701–1707.

(12) Coutre, S. E.; Barrientos, J. C.; Brown, J. R.; de Vos, S.; Furman, R. R.; Keating, M. J.; Li, D.; O'Brien, S. M.; Pagel, J. M.; Poleski, M. H.; Sharman, J. P.; Yao, N.-S.; Zelenetz, A. D. Management of Adverse Events Associated with Idelalisib Treatment - Expert Panel Opinion. *Leuk. Lymphoma* **2015**, *56*, 2779-2786.

(13) Terstiege, I.; Perry, M.; Petersen, J.; Tyrchan, C.; Svensson, T.; Lindmark, H.; Öster, L. Discovery of Triazole Aminopyrazines as a Highly Potent and Selective Series of PI3Kδ Inhibitors. *Bioorg. Med. Chem. Lett.* **2016**, *27*, 679–687.

(14) El-Sherbiny, I. M.; El-baz, N. M.; Yacoub, M. H. Inhaled Nano- and Microparticles for Drug Delivery. *Global Cardiol. Sci. Pract.* **2015**, *2015*, 2.

(15) Cushing, T. D.; Metz, D. P.; Whittington, D. A.; McGee, L. R. PI3Kδ and PI3Kγ as Targets for Autoimmune and Inflammatory Diseases. *J. Med. Chem.* **2012**, *55*, 8559–8581.

(16) Knight, Z. A.; Gonzalez, B.; Feldman, M. E.; Zunder, E. R.; Goldenberg, D. D.; Williams, O.; Loewith, R.; Stokoe, D.; Balla, A.; Toth, B.; Balla, T.; Weiss, W. A.; Williams, R. L.; Shokat, K. M. A Pharmacological Map of the PI3-K Family Defines a Role for p110alpha in Insulin Signaling. *Cell* **2006**, *125*, 733–747.

(17) Sutherlin, D. P.; Baker, S.; Bisconte, A.; Blaney, P. M.; Brown, A.; Chan, B. K.; Chantry, D.; Castanedo, G.; Depledge, P.; Goldsmith, P.; Goldstein, D. M.; Hancox, T.; Kaur, J.; Knowles, D.; Kondru, R.; Lesnick, J.; Lucas, M. C.; Lewis, C.; Murray, J.; Nadin, A. J.; Nonomiya, J.; Pang, J.; Pegg, N.; Price, S.; Reif, K.; Safina, B. S.; Salphati, L.; Staben, S.; Seward, E. M.; Shuttleworth, S.; Sohal, S.; Sweeney, Z. K.; Ultsch, M.; Waszkowycz, B.; Wei, B. Potent and Selective Inhibitors of PI3Kδ: Obtaining Isoform Selectivity from the Affinity Pocket and Tryptophan Shelf. *Bioorg. Med. Chem. Lett.* **2012**, *22*, 4296–4302.

(18) Sadhu, C.; Masinovsky, B.; Dick, K.; Sowell, C. G.; Staunton, D. E. Essential Role of Phosphoinositide 3-Kinase δ in Neutrophil Directional Movement. *J. Immunol.* **2003**, *170*, 2647–2654.

(19) Zhao, X.; Li, T.; Zhou, Z.; Chen, L.; Liu, Q.; Wang, X.; Yang, L.; Rong, Y.; Tan, R.; Yu, C.; Jiang, L.; Liu, Y.; Linghu, L.; Sun, J.; Wang, W. Certain Protein Kinase Inhibitors. WO2016066142(A1). 2016.

(20) Emtenaes, H; Alderin, L; Almqvist, F. An Enantioselective Ketene-Imine Cycloaddition Method for Synthesis of Substituted Ring-Fused 2-Pyridinones. *J. Org. Chem.* **2001**, *66*, 6756–6761.

(21) Bengtsson, C.; Almqvist, F. Regioselective Halogenations and Subsequent Suzuki-Miyaura Coupling onto Bicyclic 2-Pyridones. *J. Org. Chem.* **2010**, *75*, 972–975.

(22) Hochhaus, G.; Möllmann, H.; Derendorf, H.; Gonzalez-Rothi, R. J. Pharmacokinetic/pharmacodynamic Aspects of Aerosol Therapy Using Glucocorticoids as a Model. *J. Clin. Pharmacol.* **1997**, *37*, 881–892.

(23) Hochhaus, G.; Gonzalez-Rothi, R. J.; Lukyanov, A.; Derendorf, H.; Schreier, H.; Dalla Costa, T. Assessment of Glucocorticoid Lung Targeting by Ex-Vivo Receptor Binding Studies in Rats. *Pharm. Res.* **1995**, *12*, 134–137.

(24) Cooper, A.E. Ferguson, D. and G. K. Optimisation of DMPK by the Inhaled Route. Challenges Approaches *Curr. Drug Metab.* **2012**, *13*, 457–473.

(25) Austin, R. P.; Barton, P.; Bonnert, R. V; Brown, R. C.; Cage, P. A.; Cheshire, D. R.; Davis, A. M.; Dougall, I. G.; Ince, F.; Pairaudeau, G.; Young, A. QSAR and the Rational Design of Long-Acting Dual D 2 -Receptor / 2 -Adrenoceptor Agonists Approach to Compound Design *J. Med. Chem.* **2003**, *46*, 3210–3220.

(26) Connolly, S.; Alcaraz, L.; Bailey, A.; Cadogan, E.; Christie, J.; Cook, A. R.; Fisher, A. J.; Hill, S.; Humphries, A.; Ingall, A. H.; Kane, Z.; Paine, S.; Pairaudeau, G.; Stocks,

M. J.; Young, A. Design-Driven LO: The Discovery of New Ultra Long Acting Dibasic β2-Adrenoceptor Agonists. *Bioorg. Med. Chem. Lett.* **2011**, *21*, 4612–4616.

(27) Mindell, J. A. Lysosomal Acidification Mechanisms. *Annu. Rev. Physiol.* **2012**, *74*, 69–86.

(28) Barnden, M. J.; Allison, J.; Heath, W. R.; Carbone, F. R. Defective TCR Expression in Transgenic Mice Constructed Using cDNA-Based Alpha- and Bold Beta-Chain Genes under the Control of Heterologous Regulatory Elements. *Immunol. Cell Biol.* **1998**, *76*, 34–40.

(29) Meyuhas, O.; Dreazen, A. Chapter 3 Ribosomal Protein S6 Kinase: From TOP mRNAs to Cell Size. *Prog. Mol. Biol. Transl. Sci.* **2009**, *90,* 109-153.

(30) Beger, J.; Schöde, D.; Vogel, J. Dreikomponentenreaktionen. II. Nucleophile Substitutionen an N-(β-Haloalkyl)-Imidhalogeniden die Darstellung von Δ 2 -Oxazolinen, Δ 2 -Thiazolinen und Δ 2 -Imidazolinen. *J. Prakt. Chem. (Weinheim, Ger.)* **1969**, *311*, 408–419.

(31) Clark, J.; Bahman Parvizi, R. C. Heterocyclic Studies. Part XXXXIX. Ring Cleavage of Some Pyrimidine Derivatives in Alkalai. *J. Chem. Soc., Perkin Trans. 1 (1972-1999)* **1976**, *9*, 1004–1007.

(32) Bruno, N. C.; Tudge, M. T.; Buchwald, S. L. Design and Preparation of New Palladium Precatalysts for C-C and C-N Cross-Coupling Reactions. *Chem. Sci.* **2013**, *4*, 916–920.

(33) Callahan, J. F., Li, Tindy, Wan, Zehong, Yan, H. Preparation of pyrazolo[3,4-b] pyridine Dual Pharmacophores as PDE4-muscarinic Antagonists. WO2009100169, 2009.

(34) Bäckström, E.; Boger, E.; Lundqvist, A.; Hammarlund-Udenaes, M.; Fridén, M. Lung Retention by Lysosomal Trapping of Inhaled Drugs Can Be Predicted In Vitro With Lung Slices. *J. Pharm. Sci.* **2016**, *105*, 3432–3439.

Table of Contents Graphic

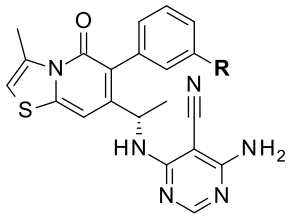	**R**			
		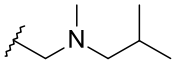	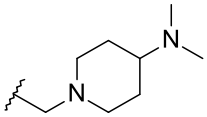	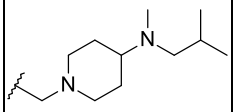
PI3Kδ enzyme pIC_{50}	9.4	9.3	9.3	9.2
PI3Kδ cell pIC_{50}	9.1	8.8	8.0	8.9
Lung t½ (h)	<0.1	2.3	23.2	9.9

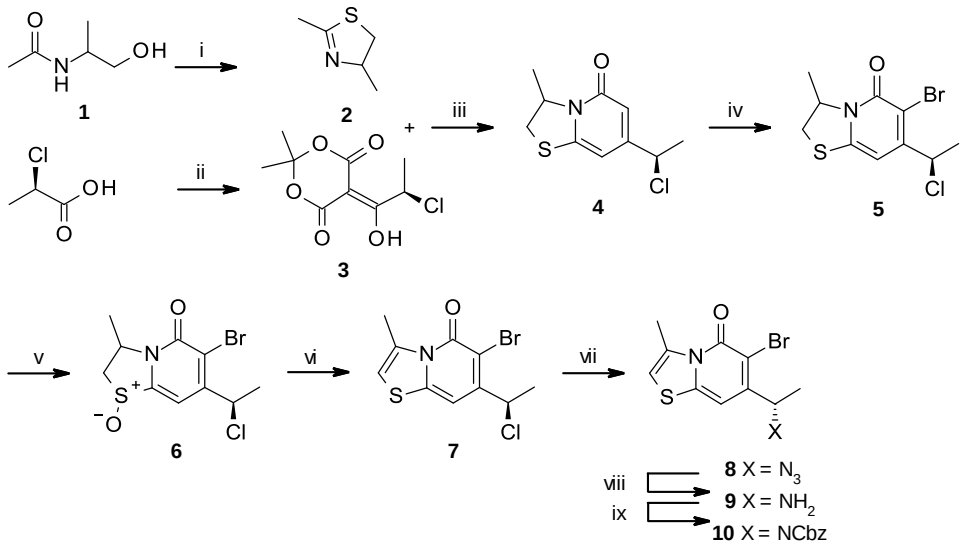
i
ii
iii
iv
v
vi
vii
viii
ix
1
2
3
4
5
6
7
8 X = N3
9 X = NH2
10 X = NCbz

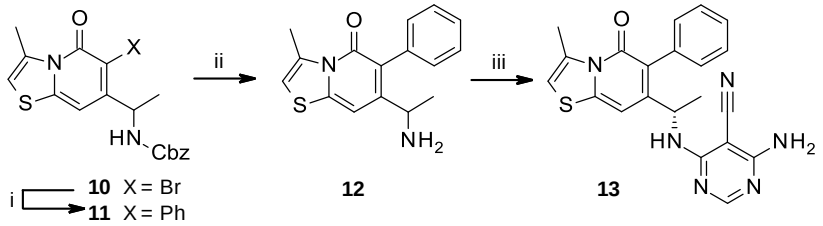
O
X
N
S
HN
Cbz
ii
O
N
S
NH2
iii
O
N
S
HN
N
NH2
N
N
i
10 X = Br
11 X = Ph
12
13

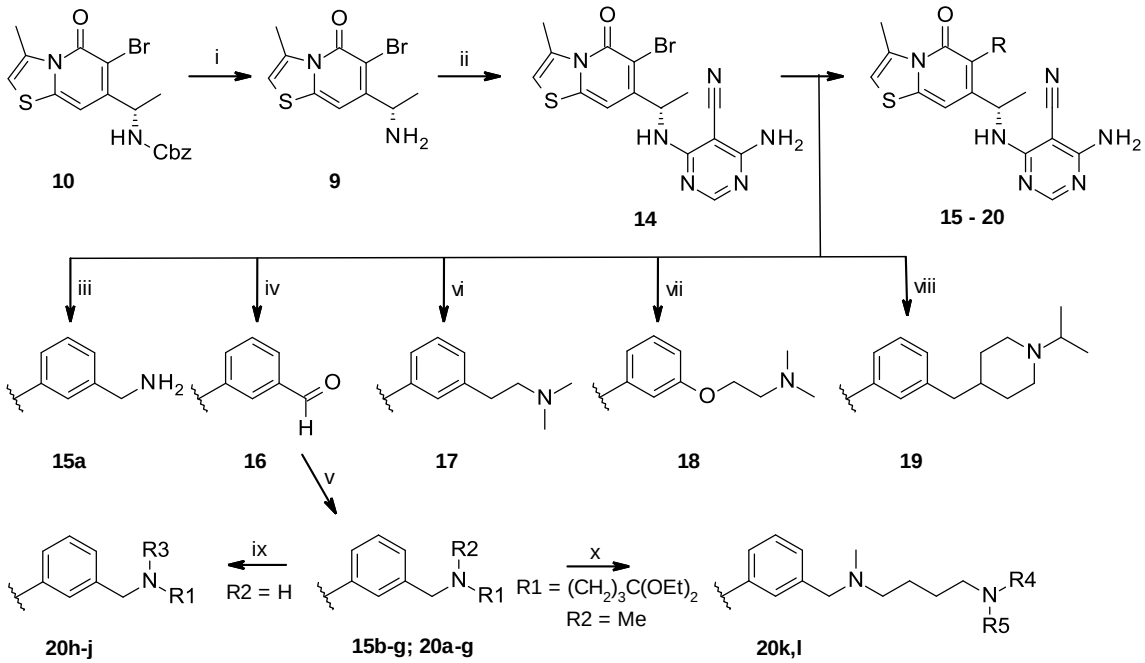
10
9
14
15 - 20
15a
16
17
18
19
20h-j
15b-g; 20a-g
20k,l
i
ii
iii
iv
v
vi
vii
viii
ix
x
R2 = H
R1 = (CH2)3C(OEt)2
R2 = Me

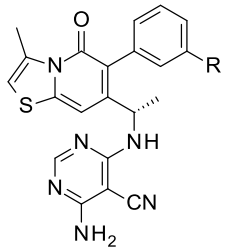

13, 15a-g

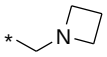
*
N

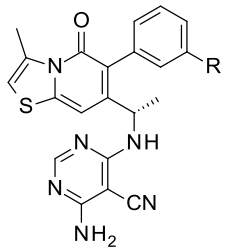

15c, 17-19

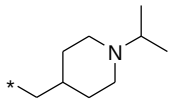
N
*

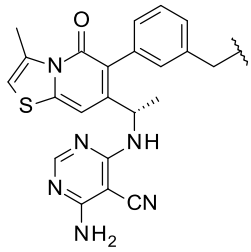

20a-l

20a

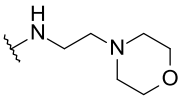

20b

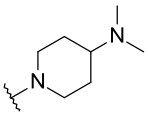

20c

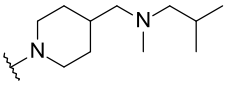

20d

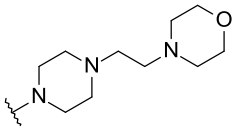

20e

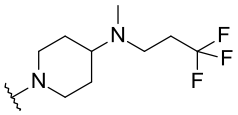

20f

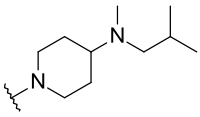

20g

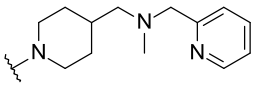

20h

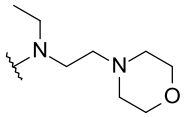

20i

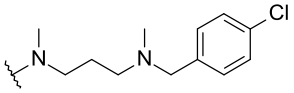

20j

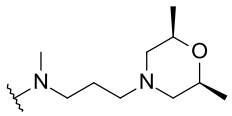

20k

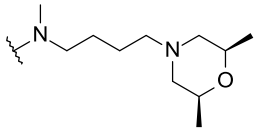

20l

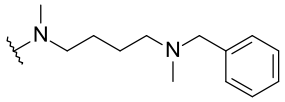

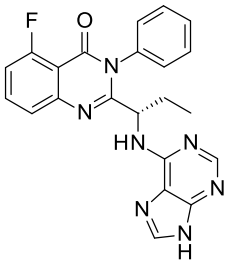

A

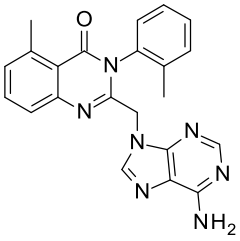

B

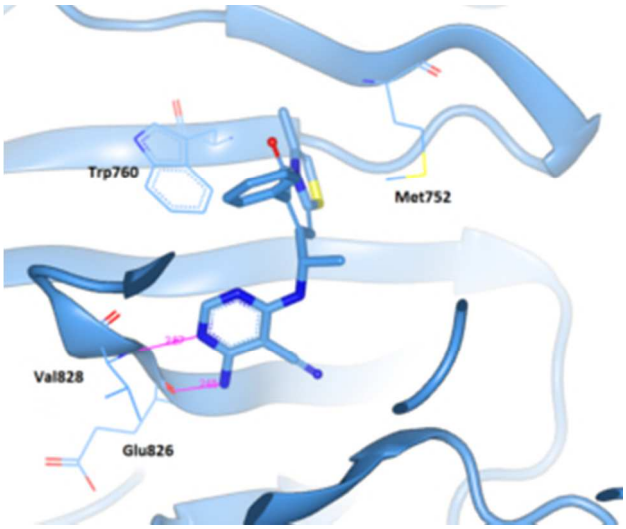

Compound **13** bound in murine PI3Kd showing the ATP binding pocket with the induced pocket between Trp760 and Met752 and with hydrogen bonds to the NH of Val828 and the carbonyl of Glu826 making the hinge interaction.

84x69mm (93 x 94 DPI)

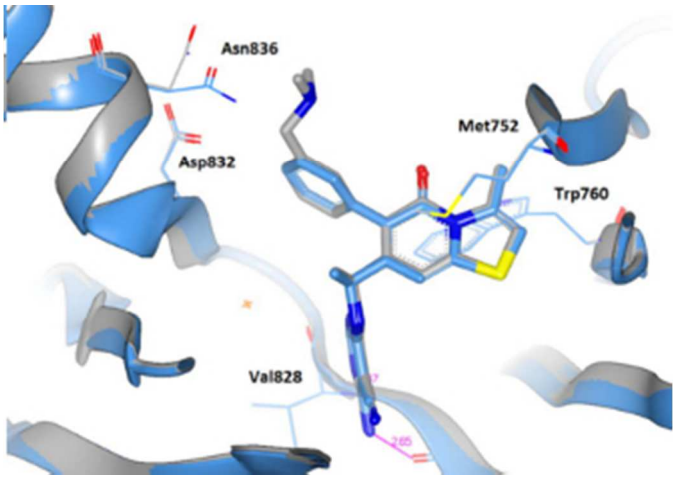

View of **15c** (grey) overlayed with **13** (blue) showing the very similar conformations adopted by the ligands and the almost identical protein conformations. Note the movement of the sidechain amide of Asn836 permitting the dimethylamino group to be accommodated.

84x59mm (100 x 100 DPI)

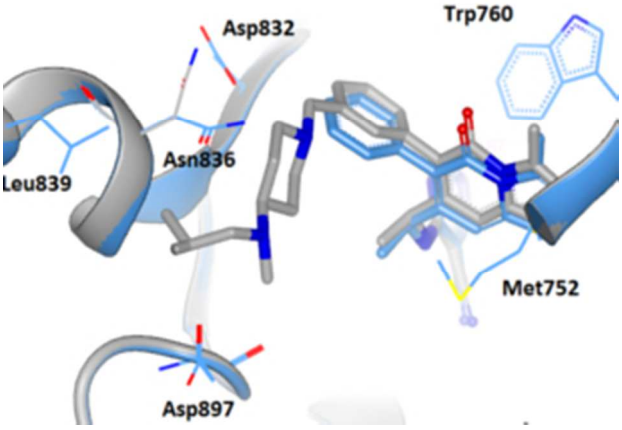

Docked structure of **20f** (grey) overlaid with **13** (blue) in murine PI3K showing the large substituted aminopiperidine accommodated in the solvent channel.

83x61mm (93 x 94 DPI)

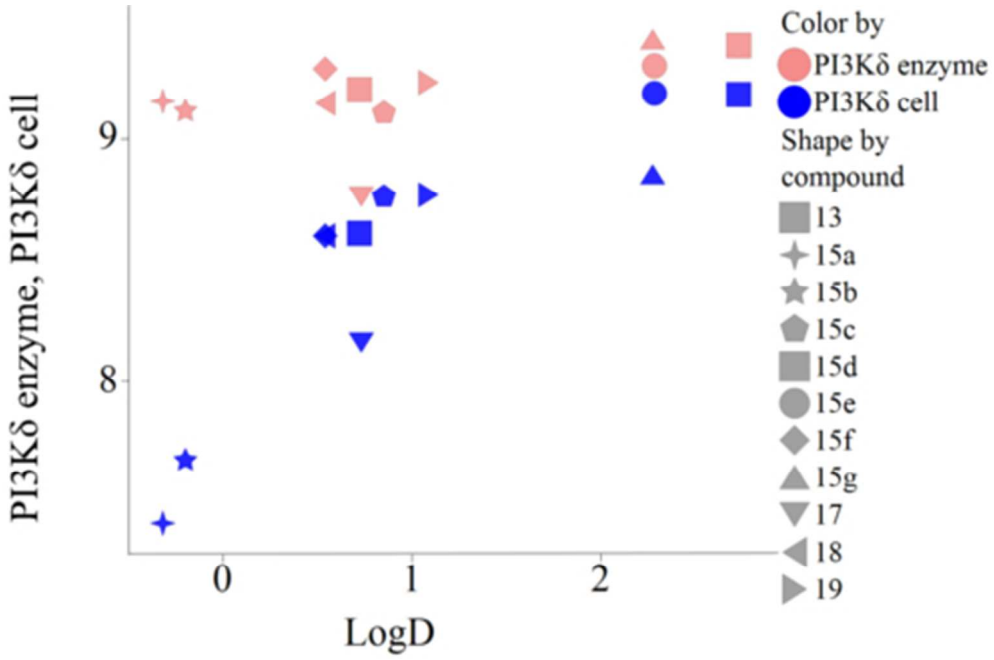

Enzyme and cell potencies for compounds **13**, **15a-g**, **17**, **18**, **19** showing cell drop-off at low lipophilicity.

84x55mm (150 x 150 DPI)

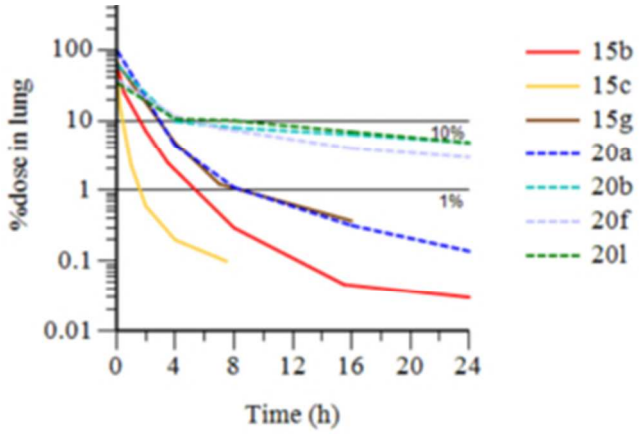

Rat ITPK time-course profiles of selected examples.

84x56mm (96 x 96 DPI)

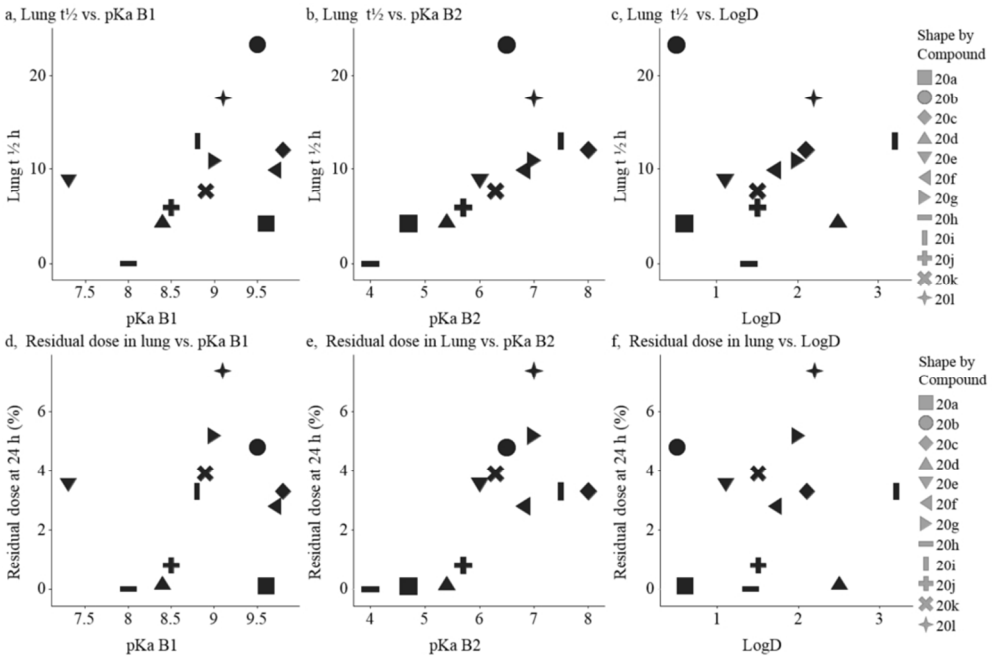

Relationships between lung retention (% remaining at 24 h; half-life) and the first and second pKas or Lipophilicity (LogD) for dibases **20a-l**.

177x115mm (150 x 150 DPI)

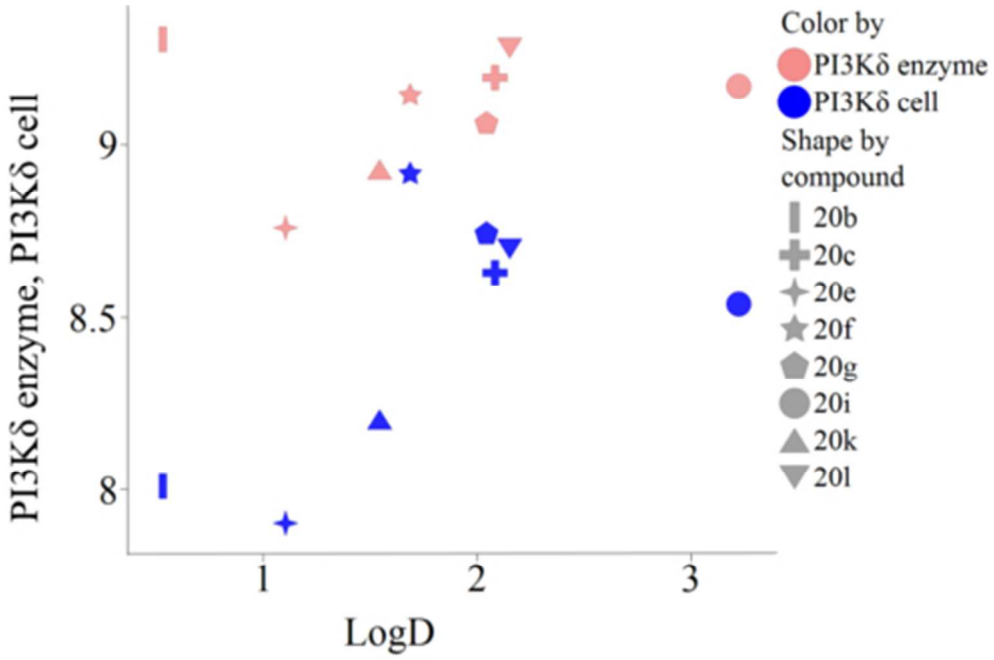

Cell drop-off for dibases.

84x55mm (150 x 150 DPI)

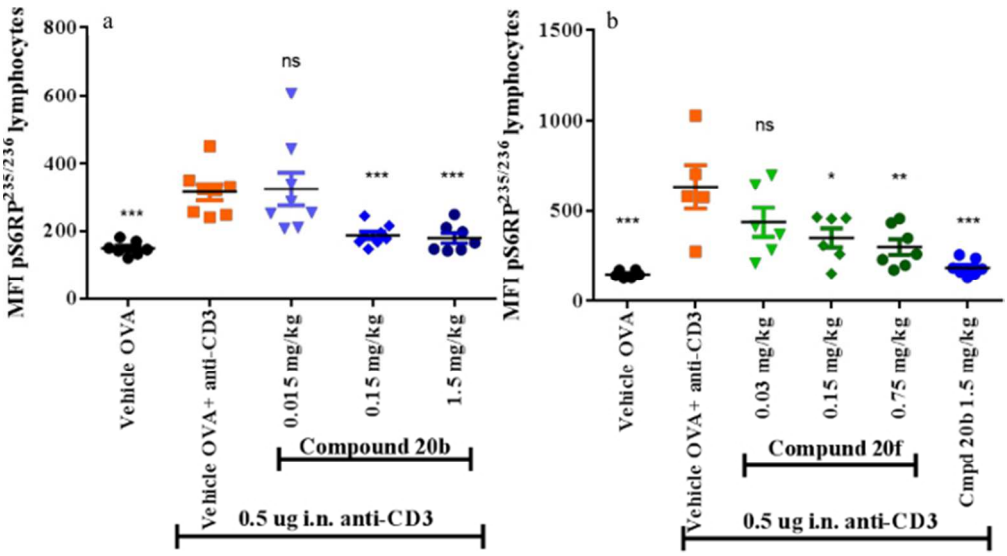

Inhibition of pS6RP in lung lavage after anti-CD3 challenge to OTII mice. **9a** compound **20b** **9b** compound **20f**. Target engagement of PI3Kδ activity is shown through measurements of pS6RP in bronchoalveolar lung lavage cells after anti-CD3 challenge to OVA-challenged OTII mice. Phosphorylation of S6RP, measured using phosphospecific antibodies, was significantly inhibited by both **20b** (9a) and **20f** (9b) in a dose-dependent manner, however the inhibition by **20b** showed better potency. Data is shown as results for individual animals at each dose with the statistical significance indicated as follows above the columns : p<0,001 ***; p<0,005 **; p<0,05 *

177x96mm (100 x 100 DPI)

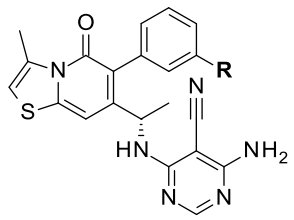	R			
		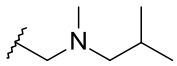	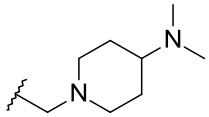	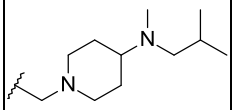
PI3Kδ enzyme pIC_{50}	9.4	9.3	9.3	9.2
PI3Kδ cell pIC_{50}	9.1	8.8	8.0	8.9
Lung t½ (h)	<0.1	2.3	23.2	9.9